

# Model-independent analysis of Higgs spin and CP properties in the process $e^+e^- \rightarrow t\bar{t}\Phi$

R.M. Godbole<sup>\*a,b</sup>, C. Hangst<sup>c</sup>, M. Mühlleitner<sup>c</sup>, S.D. Rindani<sup>d</sup> and P. Sharma<sup>d</sup>

<sup>a</sup>*Theory Division, CERN TH-PH, CH-1211, Geneva 23, Switzerland*

<sup>b</sup>*Institute for Theoretical Physics and Spinoza Institute, Utrecht University, 3508 TD Utrecht, The Netherlands*

<sup>c</sup>*Institut für Theoretische Physik, Karlsruhe Institute of Technology, 76128 Karlsruhe, Germany*

<sup>d</sup>*Theoretical Physics Division, Physical Research Laboratory, Navrangpura, Ahmedabad 380 009, India*

## Abstract

In this paper we investigate methods to study the  $t\bar{t}$  Higgs coupling. The spin and CP properties of a Higgs boson are analysed in a model-independent way in its associated production with a  $t\bar{t}$  pair in high-energy  $e^+e^-$  collisions. We study the prospects of establishing the CP quantum numbers of the Higgs boson in the CP-conserving case as well as those of determining the CP-mixing if CP is violated. We explore in this analysis the combined use of the total cross section and its energy dependence, the polarisation asymmetry of the top quark and the up-down asymmetry of the antitop with respect to the top-electron plane. We find that combining all three observables remarkably reduces the error on the determination of the CP properties of the Higgs Yukawa coupling. Furthermore, the top polarisation asymmetry and the ratio of cross sections at different collider energies are shown to be sensitive to the spin of the particle produced in association with the top quark pair.

---

\*On leave of absence from: Center for High Energy Physics, Indian Institute of Science, Bangalore 560 012, India

# 1 Introduction

One of the major goals of the LHC is to probe if the Higgs mechanism [1–3] is at the origin of electroweak symmetry breaking (EWSB). Whereas at the LHC [4] a Standard Model (SM) Higgs boson can be found in the whole canonical mass range and first information on its properties will be available, the clean environment of the International Linear Collider (ILC) [5] would be needed in order to determine the particle properties with sufficient precision. The interplay of the information available from both colliders will provide us with a clearer picture of the dynamics behind the creation of the masses of the fundamental particles [6]. This requires the determination of the spin  $J$  and the CP quantum numbers of the observed state, the measurement of its couplings to gauge bosons and fermions and finally the extraction of the trilinear and quartic Higgs self-couplings [7] to reconstruct the Higgs potential itself.

The SM Higgs boson is predicted to be CP-even and have spin zero, *i.e.*  $J^{CP} = 0^{++}$ . Should extensions beyond the SM (BSM) be realised, the existence of more than one spin zero particle is possible. Some of these particles can have CP-odd properties or even be states with no definite CP quantum number. Supersymmetric theories [8, 9] for example require the introduction of at least two complex Higgs doublets. In the Minimal Supersymmetric Extension of the Standard Model (MSSM) [3, 10] this leads after electroweak symmetry breaking to five physical Higgs states, out of which three are neutral, two CP-even and one CP-odd. Should CP violation beyond the one of the SM be provided by the Higgs sector, this would imply Higgs states with mixed CP properties. CP violation is one of the conditions to explain the Baryon Asymmetry in the Universe [11]. A study of the CP properties of the Higgs boson can hence already give some clues to BSM physics [12]. Such a study at the current and future colliders [13] would have to establish the CP properties of the observed spin 0 particle(s) and determine the amount of CP-mixing in case of CP violation. This can be done by establishing the tensor structure of the Higgs couplings to  $Z$  or  $W$  pairs and of the  $f\bar{f}\Phi$  couplings, where  $\Phi$  denotes a general  $J = 0$  state. Any deviation from the SM prediction can then be interpreted in the framework of a given model.

In the SM, the largest Higgs boson couplings are the ones to the heaviest fermions and to a massive  $W$  or  $Z$  gauge boson pair. Therefore Higgs production via these couplings or its decays into a heavy  $f\bar{f}$  or  $WW, ZZ$  pair provide the best processes to obtain information on its spin and parity. The couplings to a pair of photons or gluons, which proceed through loops of these particles, can be used, too. A plethora of observables, constructed out of the kinematic variables of the different particles involved in the production and decay of the Higgs boson, can provide this information. The strategy for a model-independent test and analysis is to assume the most general form of the relevant Higgs couplings consistent with Lorentz invariance and gauge invariance and explore how these couplings can be constrained by using the mentioned observables. This is usually possible by exploiting properties of kinematical distributions such as threshold effects and angular correlations in Higgs decays into  $W$  or  $Z$  pairs or production in  $\gamma\gamma$  fusion, without [12, 14–18] and with the inclusion of CP-violating effects [19–27]. In the decay channel into a  $Z$  boson pair even small signal samples, as available at the moment of Higgs discovery at the LHC, might be sufficient to draw first conclusions on the CP properties of the Higgs boson [27]. The Higgs production processes through Higgs-radiation and gauge boson fusion in  $e^+e^-$  collisions also provide observables to extract spin parity informations of the Higgs boson as well as the couplings of the Higgs boson with a gauge boson pair [16, 28–30], with CP violation included in [19, 31–33]. In addition, the azimuthal angular distribution of the two outgoing forward tagging jets in weak boson fusion and in gluon

fusion initiated processes can be used [34–36]. In vector boson fusion the CP nature of the Higgs  $VV$  ( $V = W, Z$ ) coupling is probed, whereas gluon fusion provides this information for the Higgs coupling to a top quark pair. It is found that a CP-even Higgs boson can be clearly distinguished from a CP-odd Higgs state.

The coupling of a pseudoscalar Higgs boson to a  $VV$  pair is always loop induced and hence suppressed with respect to the tree level coupling of a scalar state. As a result, the best among the different methods suggested to study the CP-mixing are those which use the couplings of a  $J = 0$  state to a pair of photons [14, 21–25] at the photon collider option [37] of the ILC, and to the heavy fermions  $t$  or  $\tau$  [38–47] at the LHC and the ILC. The advantage is that these particles couple democratically to the CP-even and the CP-odd components of the Higgs boson. As the photon collider option is the most remote one to be realized, the study of the associated production of a  $J = 0$  state with a  $f\bar{f}$  pair at the LHC or ILC or the analysis of the decays of a heavy Higgs produced via gluon fusion into a  $f\bar{f}$  pair are the most promising candidates to get unambiguous information on the CP properties of a state with indefinite CP quantum numbers.

The top quark is the heaviest fermion discovered so far and, providing the largest Yukawa coupling, plays a special role. At a future ILC Higgs boson production in association with a top quark pair,  $e^+e^- \rightarrow t\bar{t}\Phi$  [48–52] leads to sufficiently high rates [53] and can hence be used to extract CP information [41, 43–45] by exploiting angular correlations and/or the polarisation of heavy fermions [44, 45]. These can also be exploited in the Higgs decays to heavy fermions [38]. Reference [43] employs an optimal observable technique to show that the discrimination between a CP-even and a CP-odd case at a high level of statistical significance is possible with low luminosity, and that a non-zero CP-violating coupling can be determined at the  $1\sigma$  level with  $\int \mathcal{L} = 100 \text{ fb}^{-1}$ . In Ref. [44] the extraction of the Higgs CP quantum numbers in  $t\bar{t}\Phi$  production at a future ILC through the measurement of the total cross section and its energy dependence as well as of the top polarisation asymmetry has been discussed. In the current paper we extend the analysis in two ways. Firstly, we allow for more than two neutral spin 0 states while writing the most general CP-violating  $f\bar{f}\Phi$  vertex. Secondly, we investigate possible sensitivities to probe this general  $f\bar{f}\Phi$  vertex in the combined study of three different observables. The observables we use are the total cross section  $\sigma$  and its energy dependence, which has been shown to exhibit an unambiguously different behaviour for CP-even and CP-odd Higgs bosons, the top quark polarisation asymmetry  $P_t$  and the up-down asymmetry  $A_\phi$  of the antitop quark with respect to the top-electron plane. The latter can directly probe CP violation. We also discuss how well the energy dependence of the cross section and the top polarisation asymmetry can differentiate between the case of a spin 1 particle produced in association with a  $t\bar{t}$  pair and that of a spin 0 particle.

The outline of the paper is as follows. In section 2 we will discuss the observables and their individual sensitivities to the Higgs CP properties. Then the combination of all observables will be investigated with respect to an improvement in the determination of the CP quantum numbers. In section 3 the associated production of a spin 1 particle with a top quark pair will be discussed to investigate to what extent the total cross section and the top polarisation asymmetry can help to distinguish a spin 1 from a spin 0 state. We will conclude in section 4.

## 2 The observables

In this section we will discuss the observables for the production of an arbitrary CP-violating Higgs boson  $\Phi$  in association with a top-quark pair at a future  $e^+e^-$  linear collider,

$$e^+e^- \rightarrow t\bar{t}\Phi. \quad (1)$$

The value of the total cross section  $\sigma$  and its energy dependence exhibit sensitivity to the CP nature of the Higgs boson and allow for a distinction between a CP-odd and a CP-even Higgs boson. The top quark polarisation asymmetry  $P_t$  serves as a further observable. Both  $\sigma$  and  $P_t$  are CP-even and hence do not test CP violation. The  $t\bar{t}\Phi$  production process, however, exhibits already at tree-level CP violation in the interference between the diagrams where  $\Phi$  is emitted from the top (antitop) and where it is emitted from the  $Z$  boson [41]. The up-down asymmetry  $A_\phi$  projects out this interference term and thus tests CP violation. In the following we will discuss the observables  $\sigma$ ,  $P_t$  and  $A_\phi$  in detail as well as their sensitivity to the Higgs CP properties. We will examine if the longitudinal polarisation of the initial  $e^\pm$  beams can help to improve the sensitivity. For the degree of polarisation, the standard ILC values of  $P_{e^-} = -0.8$  and  $P_{e^+} = 0.6$  will be assumed. Positive values of  $P_{e^-}, P_{e^+}$  correspond to right-handed polarisation. Finally, we will combine all observables to derive the errors on the CP parameters in a general CP-violating  $t\bar{t}\Phi$  coupling by performing a  $\chi^2$  test.

### 2.1 The total cross section

The associated production of a SM Higgs boson with a top quark pair,  $e^+e^- \rightarrow t\bar{t}H$ , can be measured with an accuracy of  $\mathcal{O}(10)\%$  for  $M_H \lesssim 200$  GeV [53]. At tree level [48], it proceeds through the Higgs radiation off the  $t, \bar{t}$  lines and a diagram with the Higgs boson produced in association with a  $Z$  boson which then splits into a  $t\bar{t}$  pair, *cf.* Fig. 1. This diagram only contributes with a few percent as long as  $\sqrt{s} \leq 1$  TeV. In fact, the bulk of the cross section stems from the splitting of the virtual photon into  $t\bar{t}$ .

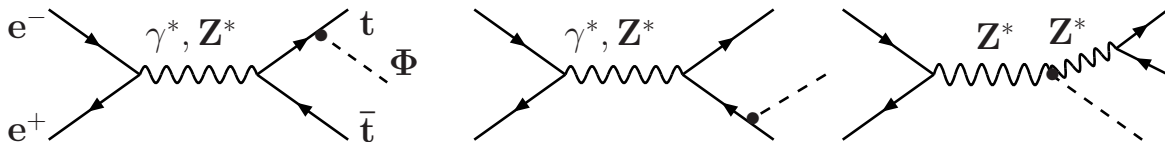


Figure 1: Feynman diagrams contributing to the associated production of a Higgs boson  $\Phi$  with a top quark pair.

In models with more than one Higgs boson as *e.g.* a general 2-Higgs doublet model (2HDM) or supersymmetric extensions of the SM, there are additional diagrams with a CP-odd (even) Higgs boson splitting into  $t\bar{t}$  for (pseudo-)scalar Higgs production. In CP-violating models both Higgs bosons are CP-mixed states, one of them splitting into a top quark pair. This contribution is in general small unless Higgs decays into  $t\bar{t}$  are kinematically allowed. We assume here that by the time the CP quantum numbers of Higgs bosons will be tested, all Higgs bosons will have been discovered and their masses will have been determined. By applying appropriate cuts on the

invariant mass of the  $t\bar{t}$  pair we can hence safely neglect these additional diagrams.<sup>1</sup>

In order to discuss a general CP-mixed Higgs state  $\Phi$  we parametrize the  $t\bar{t}\Phi$  coupling by

$$C_{t\bar{t}\Phi} = -i \frac{e}{\sin\theta_W} \frac{m_t}{2M_W} (a + ib\gamma_5) \equiv -ig_{t\bar{t}H} (a + ib\gamma_5) , \quad (2)$$

where  $\theta_W$  denotes the Weinberg angle,  $m_t$  the top quark mass and  $M_W$  the  $W$  boson mass. The coefficients  $a$  and  $b$  are assumed to be real and in the SM are given by  $a = 1, b = 0$ . A pure pseudoscalar coupling is provided by  $a = 0, b \neq 0$ . A coupling to a Higgs state with indefinite CP quantum numbers is realized if simultaneously  $a \neq 0$  and  $b \neq 0$ . The exact values of these parameters depend on the model under consideration. In the MSSM for example the Higgs couplings to up-(down-)type quarks are suppressed (enhanced) for large values of  $\tan\beta$ , the ratio of the vacuum expectation values of the two complex Higgs doublets [3, 54]. From the experimental side the upper bounds on the electric dipole moments of the neutron and the electron provide important constraints on non-standard Higgs sector CP violation [12]. Within a general 2HDM with maximal CP violation, values with  $|ab| \lesssim 2$  are in accordance with low-energy constraints [40, 55]. We work in a model-independent approach and in the following let  $a$  and  $b$  vary between  $-1$  and  $1$ , if not stated otherwise.

For the calculation of the total cross section the  $ZZ\Phi$  coupling will be needed, too. It is parametrized in terms of the SM coupling  $g_{ZZH}$  by a parameter  $c$ , *i.e.*

$$g_{ZZ\Phi}^{\mu\nu} = -ic \frac{eM_Z}{\sin\theta_W \cos\theta_W} g^{\mu\nu} \equiv -ic g_{ZZH} g^{\mu\nu} . \quad (3)$$

The  $ZZ\Phi$  coupling and hence the parameter  $c$  will be determined from other channels [4, 5, 56, 57] so that the analysis for the determination of the Higgs CP properties can be performed for a fixed value of  $c$ . In order to reduce the number of free parameters, we will choose  $c = -a$  in our analysis. This is a reasonable choice as  $c = 0$  in case of a CP-odd Higgs boson and  $|c| \leq 1$  in general<sup>2</sup>. For  $a = 1$  the  $ZZ\Phi$  coupling then takes the SM form. In principle,  $ZZ$  can also couple to the CP-odd part of the Higgs boson [59–61]. This coupling is, however, zero at tree-level and only generated through tiny loop corrections. Therefore we consider only  $ZZ\Phi$  couplings without contributions involving the CP-odd part of  $\Phi$ .

Neglecting the small contribution of the diagram involving the  $ZZ\Phi$  vertex, the differential cross section with respect to the scaled energies  $x_{1,2} = 2E_{t,\bar{t}}/\sqrt{s}$ , can be cast into the form

$$\begin{aligned} \frac{d\sigma}{dx_1 dx_2} = \frac{\alpha^2}{4\pi s} \left\{ \left[ Q_e^2 Q_t^2 + \frac{(v_e^2 + a_e^2)(v_t^2 + a_t^2)}{(1 - h_z)^2} + \frac{2Q_e Q_t v_e v_t}{1 - h_z} \right] (a^2 F_1^H + b^2 F_1^A) \right. \\ \left. + \frac{v_e^2 + a_e^2}{(1 - h_z)^2} a_t^2 (a^2 F_2^H + b^2 F_2^A) \right\} g_{t\bar{t}H}^2 , \quad (4) \end{aligned}$$

where  $\alpha^{-1} = \alpha^{-1}(s) \sim 128$ ,  $h_z = M_Z^2/s$  and  $v_f = (2I_f^{3L} - 4Q_f s_W^2)/(4s_W c_W)$ ,  $a_f = 2I_f^{3L}/(4s_W c_W)$  are the usual  $Zf\bar{f}$  couplings given in terms of the fermion charge  $Q_f$  and the third component of the

<sup>1</sup>In case the Higgs bosons are not discovered because of suppressed couplings to gauge bosons or too heavy masses, the process is not affected by these additional Higgs bosons either. Their influence is negligible in the first case, and they won't play any role in the second case at sufficiently low c.m. energy.

<sup>2</sup>This follows from a sum rule for the Higgs gauge coupling [58, 59] in models with a Higgs sector containing only Higgs singlets and doublets.

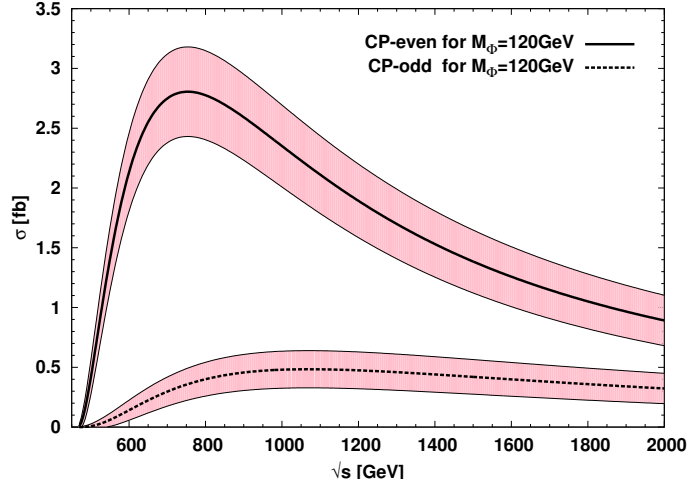


Figure 2: Total cross section in fb for SM (full) and purely CP-odd (dashed) Higgs production in association with a  $t\bar{t}$  pair as function of the c.m. energy for  $M_\Phi = 120$  GeV and unpolarised  $e^\pm$  beams. The pink (grey) band indicates the statistical error at  $\pm 5\sigma$  with  $\int \mathcal{L} = 500 \text{ fb}^{-1}$ .

weak isospin  $I_f^{3L}$  ( $f = t, e$ ). We have introduced the short-hand notation  $s_W = \sin \theta_W$ ,  $c_W = \cos \theta_W$ . The expressions for the form factors  $F_{1,2}^{H,A}$  for scalar and pseudoscalar Higgs bosons are given in Refs. [48]. Note that in the spin averaged matrix element terms proportional to the combination  $ab$  of the CP-even and CP-odd coupling parameters in the Yukawa coupling do not appear.

The total cross section is a CP-even observable and not sensitive to possible CP violation. Its threshold rise, however, is strikingly different for the scalar and pseudoscalar case as has been shown in Ref. [44]. Parametrizing the deviation  $\rho$  from the threshold by

$$\rho = 1 - \frac{2m_t}{\sqrt{s}} - \frac{M_\Phi}{\sqrt{s}}, \quad (5)$$

the latter shows a softer dependence on  $\rho$ , which is given by  $\sim \rho^3$ . The rise for a purely CP-even Higgs boson  $H$  on the other hand is  $\sim \rho^2$ . The threshold rise can hence be exploited to distinguish a pseudoscalar from a scalar Higgs boson. Taking into account only statistical fluctuations, for a 120 GeV Higgs boson an integrated luminosity of  $500 \text{ fb}^{-1}$  is sufficient to distinguish the purely pseudoscalar from the SM case at  $5\sigma$  confidence level, as can be inferred from Fig. 2. According to our coupling parametrization, here and in the following SM refers to  $a = 1, b = 0$  in the  $t\bar{t}\Phi$  coupling and purely pseudoscalar refers to  $a = 0, b = 1$ , if not stated otherwise.

In the following we discuss to what extent the value of the total cross section can be exploited to extract the CP properties of the Higgs boson. The cross section is subject to higher-order (SUSY-) QCD [49–51] and electroweak (EW) [52] corrections. The QCD corrections can be significant for collider energies near the threshold. In the continuum, for  $\sqrt{s} = 1$  TeV they are of moderate size for both the scalar and pseudoscalar Higgs boson. The EW corrections can reach about 10%. For a precise determination of the top Yukawa coupling the corrections have to be taken into account. In this analysis we neglect their influence in a first approximation. We will supplement our analysis later with the use of the polarisation asymmetry of the top quark which we expect to be less

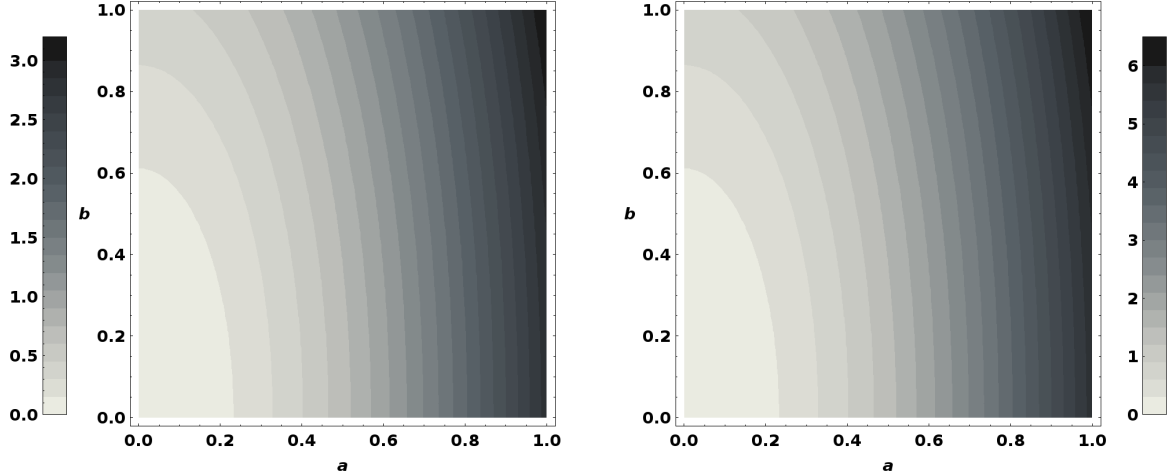


Figure 3: Contour plot of the total cross section  $\sigma(e^+e^- \rightarrow t\bar{t}\Phi)$  in fb in the  $a - b$  parameter plane for  $M_H = 120$  GeV and  $\sqrt{s} = 800$  GeV with unpolarised (left) and polarised (right)  $e^\pm$  beams. The grey code indicates the value of the cross section.

sensitive to such corrections.

The total  $t\bar{t}\Phi$  cross section values are shown for unpolarised  $e^\pm$  beams in Fig. 3 (left) as contours in the  $a - b$  plane. We have chosen  $M_\Phi = 120$  GeV and the c.m. energy  $\sqrt{s} = 800$  GeV. Note that here and in the following the diagram with the  $ZZ\Phi$  coupling is always taken into account in the numerical analyses. Since the cross section depends quadratically on  $a, b$  (for our choice of  $c = -a$ ) the contour lines are symmetric with respect to the sign of  $a$  and  $b$  so that only results for positive values of  $a$  and  $b$  are shown. The cross section decreases with decreasing values of  $a, b$ . The SM value of the cross section amounts to 2.78 fb. The cross section for a purely CP-odd Higgs boson is with 0.4 fb much smaller than the one for a SM Higgs boson, see also Fig. 2. Furthermore, the dependence on  $b$  is rather flat in contrast to the dependence on  $a$ . We hence expect the cross section to be mostly sensitive to  $a$ . Polarisation of the initial  $e^\pm$  beams can help to increase the cross section for our choice of  $P_{e^\pm}$ , as shown in Fig. 3 (right). It increases the cross section by about a factor of 2, independent of the CP nature of the Higgs boson. In the Appendix the replacements are listed, which have to be applied in the formula of the cross section in case of initial beam polarisation.

Figure 4 shows the errors on  $a, b$  extracted from the total cross section, and hence the sensitivity of this observable to the Higgs CP parameters. For the error determination we define a level of confidence  $f$  to identify the area in the  $a - b$  plane for which the value of the observable  $O(a, b)$  (here  $\sigma(a, b)$ ) cannot be distinguished from the reference value  $O(a_0, b_0)$  at a specific point  $(a_0, b_0)$ . Ignoring systematic errors, it is given by

$$|O(a, b) - O(a_0, b_0)| = f\Delta O(a_0, b_0), \quad (6)$$

where  $\Delta O(a_0, b_0)$  is the statistical fluctuation in  $O$  at an integrated luminosity  $\mathcal{L}$  chosen to be 500  $\text{fb}^{-1}$  in the following, if not stated otherwise. For the cross section it is given by

$$\Delta\sigma = \sqrt{\frac{\sigma}{\mathcal{L}}}. \quad (7)$$

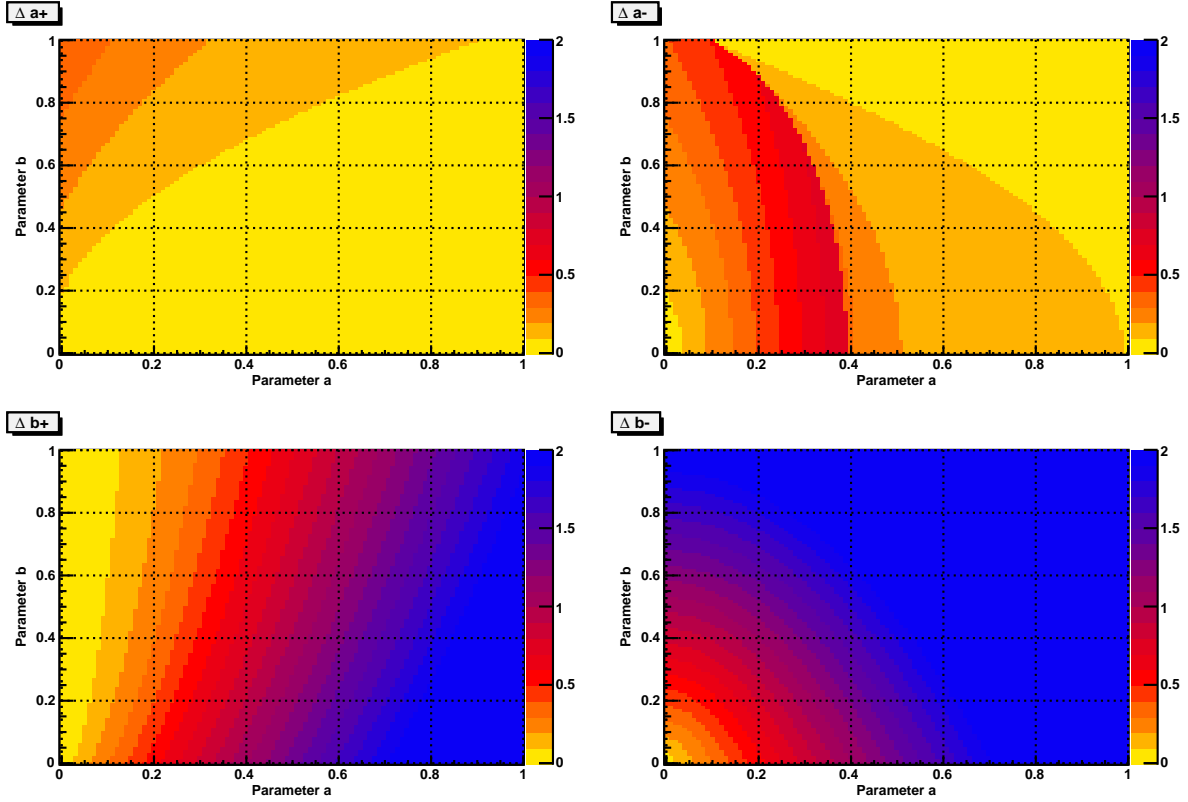


Figure 4: Errors  $\Delta a^+$  (upper left) and  $\Delta a^-$  (upper right) on  $a$  as well as  $\Delta b^+$  (lower left) and  $\Delta b^-$  (lower right) on  $b$ , extracted from the total cross section  $\sigma(e^+e^- \rightarrow t\bar{t}\Phi)$  at  $1\sigma$  confidence level for  $M_\Phi = 120$  GeV at  $\sqrt{s} = 800$  GeV with  $\int \mathcal{L} = 500$  fb $^{-1}$ . The  $e^\pm$  beams are unpolarised. The colour code indicates the magnitude of the respective error.

The errors on  $a$  and  $b$  for the point  $(a_0, b_0)$  are then determined by the maximal extensions  $\Delta a^+$  ( $\Delta a^-$ ) in positive (negative)  $a$  direction and  $\Delta b^+$  ( $\Delta b^-$ ) in positive (negative)  $b$  direction, necessary to reach the area outside the thus defined range of insensitivity.

As anticipated from the strong dependence of the cross section on  $a$  and as can be inferred from the figure, the cross section is very sensitive to  $a$ . In most of the parameter range  $a$  can be determined with an accuracy of 0.2 or better. The error  $\Delta a^-$  is large for  $a \lesssim 0.4$ . This can be understood by realizing that the area of insensitivity at  $1\sigma$  for a point  $(a_0, b_0)$  in this parameter region is given by an elliptic band in the  $(a, b)$  plane around this point. Since the value of  $b$  is not known a priori from any other measurement, the area outside the band of insensitivity is only reached for large  $\Delta a^-$ . An illustrative example is shown in Fig. 5 (left). For  $a \gtrsim 0.4$  the insensitive area cuts the edge of the parameter space  $|b| \leq 1$ , so that the error  $\Delta a^-$  is smaller, *cf.* Fig. 5 (right). The sensitivity to  $b$  is only good where the influence of the dominant contribution to the cross section from terms proportional to  $a$  is small. This is obviously the case for small  $a$  values. The total cross section can therefore be exploited to determine the CP-even part of a  $t\bar{t}\Phi$  coupling. From the discussion concerning  $\Delta a^-$  we expect that the sensitivity on  $a$  will significantly improve if  $b$  can be constrained from other observables. We furthermore found that polarised  $e^\pm$  beams improve the sensitivity only marginally.



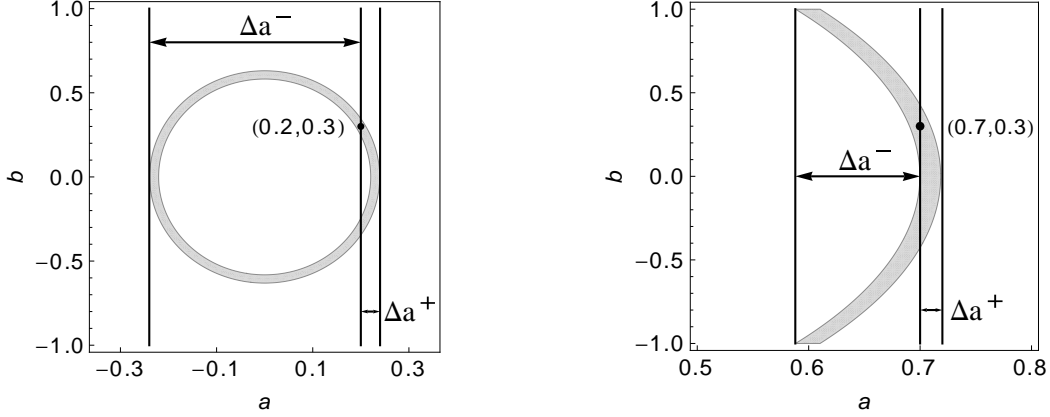


Figure 5:  $1\sigma$  band of insensitivity for  $(a_0, b_0) = (0.2, 0.3)$  (left) and  $(a_0, b_0) = (0.7, 0.3)$  (right). The corresponding errors  $\Delta a^+$ ,  $\Delta a^-$  are indicated in the figures. The errors  $\Delta b^\pm$  are derived analogously

## 2.2 The polarisation asymmetry of the top quark

Since the top decay width is large ( $\Gamma_t \sim 1.5$  GeV) the top quark decays much before hadronization. Its spin information is hence translated to the distributions of the decay products and not contaminated by strong interaction effects. As the lepton angular distribution in the decay  $t \rightarrow bW \rightarrow bl\nu$  is not affected by any non-standard effects in the decay vertex, it is a pure probe of the physics associated with the top quark production process [22, 62]. Thus the polarisation asymmetry  $P_t$  of the top quark is another observable expected to probe the Higgs CP properties. Both for polarised and unpolarised  $e^\pm$  beams it is given by

$$P_t = \frac{\sigma(t_L) - \sigma(t_R)}{\sigma(t_L) + \sigma(t_R)}, \quad (8)$$

where  $t_{L,R}$  denotes a left-, right-handed top quark. Note that, since  $P_t$  is a CP-even quantity, the polarisation asymmetry of the anti-top is the same as  $P_t$  but with opposite sign. The cross section for an  $L$ -,  $R$ -polarised top quark can be decomposed into a term  $\sigma_0$  proportional to the spin-averaged cross section and a term  $\sigma_1$  proportional to the helicity of the top quark,

$$\sigma_{L,R} = \sigma_0 - \lambda\sigma_1, \quad \lambda = -1, +1 \quad \text{for } L, R, \quad (9)$$

with the total cross section given by

$$\sigma(t\bar{t}\Phi) = 2\sigma_0. \quad (10)$$

We can hence express  $P_t$  as

$$P_t = \frac{2\sigma_1}{2\sigma_0}, \quad (11)$$

where the differential cross section corresponding to  $\sigma_1$ , neglecting the small contribution of the diagram involving the  $ZZ\Phi$  vertex, is given by

$$\frac{d\sigma_1}{dx_1 dx_2} = \frac{\alpha^2}{4\pi s} a_t g_{ttH}^2 \left[ \frac{Q_e Q_t v_e}{1 - h_z} + \frac{(a_e^2 + v_e^2) v_t}{(1 - h_z)^2} \right] (a^2 G^H + b^2 G^A), \quad (12)$$

with the form factors

$$\begin{aligned}
G^H(x_1, x_2) = & P(2 - x_1 - x_2) \left\{ x_1(1 - x_1)(x_1 - x_2)(1 - x_2) - 16h_t^2(2 - x_1 - x_2) \right. \\
& - 2h_t[4 + x_1(-3 + x_1)(2 + x_1) - 6x_2 + 8x_1x_2 + (1 - x_1)x_2^2] + h_\Phi[x_1(x_2 - x_1) \\
& \left. + 4h_t(2 - x_1 - x_2)] \right\}
\end{aligned} \tag{13}$$

and

$$\begin{aligned}
G^A(x_1, x_2) = & P(x_1 - x_2)(2 - x_1 - x_2) \left\{ h_\Phi(4h_t + x_1) + (1 - x_1)[x_1(1 - x_2) \right. \\
& \left. - 2h_t(2 - x_1 - x_2)] \right\}.
\end{aligned} \tag{14}$$

We have introduced the prefactor

$$P = \frac{1}{\sqrt{1 - \frac{4h_t}{x_1^2}(1 - x_1)^2x_1(1 - x_2)^2}} \tag{15}$$

and  $h_\Phi = M_\Phi^2/s$ ,  $h_t = m_t^2/s$ . Since  $P_t$  is given by a ratio of cross sections, this quantity has the advantage of being independent of an overall model-dependent normalization of the  $t\bar{t}\Phi$  coupling.

The total cross section  $\sigma$  and the helicity projected cross section  $2\sigma_1$  are shown in Fig. 6 (left) and (right), respectively, as a function of  $\sqrt{s}$  for a scalar SM Higgs and a purely pseudoscalar Higgs and for two different Higgs masses  $M_\Phi = 120$  and  $150$  GeV. Like in the case of the total cross section,  $\sigma_1$  shows a flat threshold rise for the pseudoscalar and a steep one for the scalar Higgs. The dependence on  $\rho$ , which parametrizes the small deviation from the threshold c.m. energy, differs by approximately one power for the CP-even and the CP-odd case, like in the case of  $\sigma = 2\sigma_0$ . This results in a threshold rise for  $P_t$  which is approximately the same for the scalar and the pseudoscalar Higgs as can be inferred from Fig. 7. Due to the reduced phase space the cross section and the top

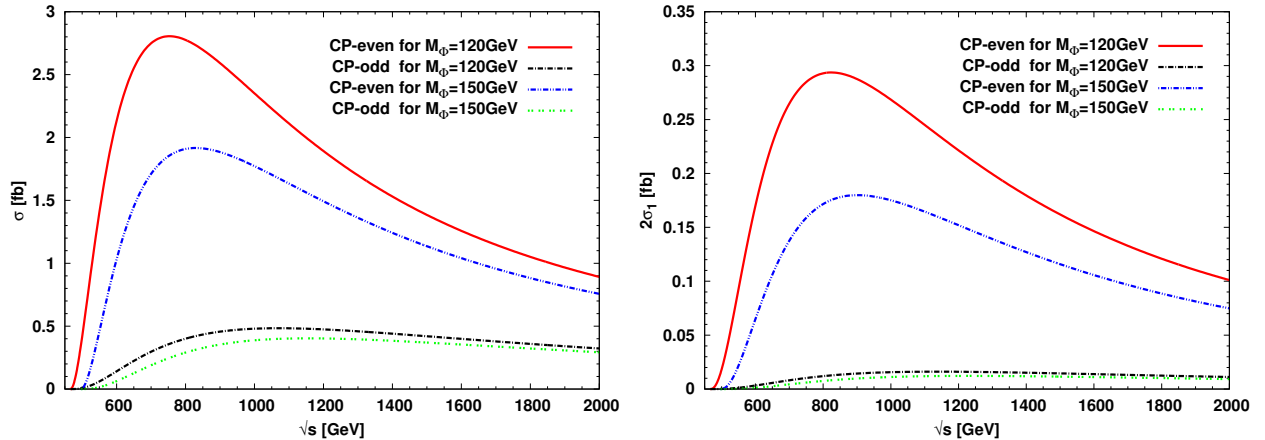


Figure 6: The total cross section  $\sigma$  (left) and the helicity projected cross section  $2\sigma_1$  (right) for a SM and a purely pseudoscalar Higgs boson as a function of  $\sqrt{s}$  for two masses  $M_\Phi = 120$  and  $150$  GeV with unpolarised  $e^\pm$  beams.

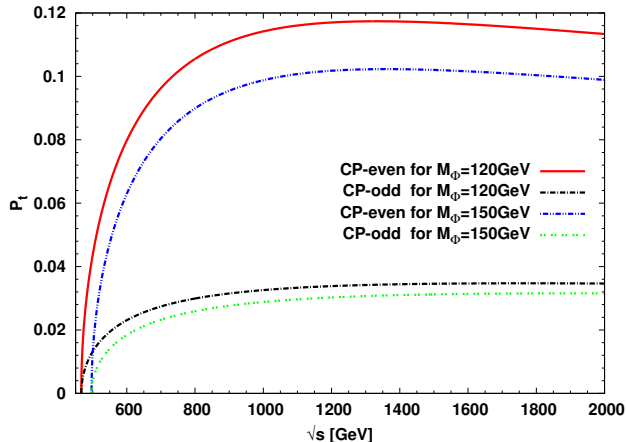


Figure 7: The top polarisation asymmetry for a SM and a purely pseudoscalar Higgs boson as a function of  $\sqrt{s}$  for two masses  $M_\Phi = 120$  and  $150$  GeV with unpolarised  $e^\pm$  beams.

polarisation asymmetry decrease with increasing Higgs mass.

Furthermore, the values of  $\sigma_0$ ,  $\sigma_1$  and of  $P_t$  are very different depending on the CP quantum numbers of the spin 0 state. The difference is solely due to different form factors  $F_{1,2}^H, F_{1,2}^A$  ( $G^H, G^A$ ) for the scalar and pseudoscalar Higgs in  $\sigma_0$  ( $\sigma_1$ ). There is no difference in the coupling structure for the scalar  $H$  and the pseudoscalar  $A$ , *cf.* Eqs. (4) and (12). At very high energies, the chiral limit is reached and the form factors for  $H$  and  $A$  (and hence the corresponding values of  $\sigma_0$  and  $\sigma_1$ ) become equal for a scalar and a pseudoscalar Higgs, up to the contributions from the diagram with the  $ZZ\Phi$  coupling, which are subleading at high c.m. energy. This behaviour can be anticipated from Figs. 6 (left) and (right). For the polarisation asymmetry, being the ratio of  $\sigma_0$  and  $\sigma_1$ , the chiral limit is reached much more slowly. We also studied this behaviour of  $P_t$  at high energies in the process  $e^+e^- \rightarrow b\bar{b}\Phi$  which, apart from the couplings and masses, is identical to  $t\bar{t}\Phi$  production. Due to the smaller final state masses, however, the process takes place at lower energies and the chiral limit can be observed at much lower energies compared to the  $t\bar{t}\Phi$  final state.

The values of  $P_t$  are shown as contour plots in the  $a - b$  parameter plane in Fig. 8 for  $M_\Phi = 120$  GeV,  $\sqrt{s} = 800$  GeV and unpolarised  $e^\pm$  beams. The top polarisation asymmetry in case of a purely pseudoscalar state is with 0.03 much smaller than the one for a SM Higgs boson with 0.11. Furthermore,  $P_t$  rapidly increases with  $a$  for large values of  $b$  and small values of  $a$  and then approaches a nearly constant behaviour in  $a$ . For small  $b$ ,  $P_t$  is constant in  $a$  (due to our choice  $c = -a$ ), as the  $b$  contribution to  $\sigma_0$  and  $\sigma_1$  does not play a role and can be neglected. The coupling factor  $a^2$  hence cancels in the ratio of  $\sigma_1$  and  $\sigma_0$  so that  $P_t$  is simply given by the corresponding ratio of the form factors and is independent of  $a$ . The same of course holds for small values of  $a$ . Here  $P_t$  is almost constant in  $b$ . Overall, the change of  $P_t$  with  $b$  is small. The largest values of  $P_t$  are reached for large  $a$ . Polarising the  $e^\pm$  beams increases  $P_t$  independently of the CP nature of the Higgs boson by roughly a factor of 3. The replacements to be made in the formulae of  $\sigma_0, \sigma_1$  for polarised beams are given in the Appendix.

The errors on the extraction of  $a$  and  $b$  from the top polarisation asymmetry have been calculated as well, with  $\Delta O(a_0, b_0)$  of Eq. (6) given by

$$\Delta O(a_0, b_0) = \Delta P_t = \frac{1}{\sqrt{\sigma\mathcal{L}}} \sqrt{1 - P_t^2}. \quad (16)$$

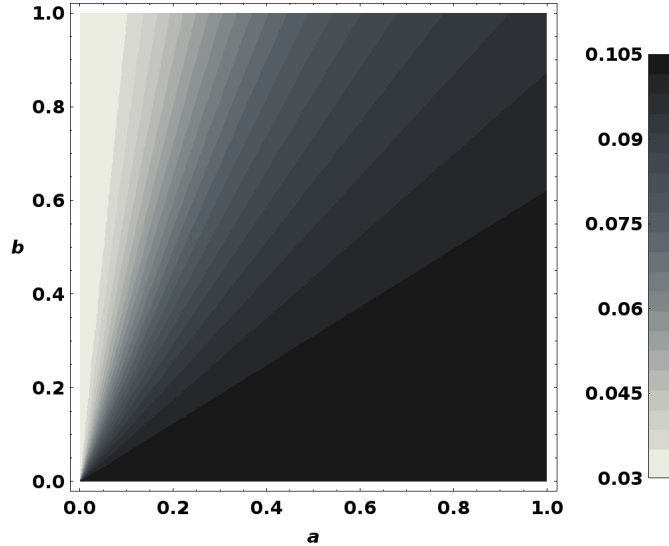


Figure 8: Contour plot of the top polarisation asymmetry  $P_t$  in the  $a - b$  parameter plane for  $M_H = 120$  GeV and  $\sqrt{s} = 800$  GeV. The  $e^\pm$  beams are unpolarised. The grey code indicates the value of  $P_t$ .

The errors on  $a$  and  $b$  for unpolarised beams turn out to be larger than 1. Polarisation only slightly improves the situation. Whereas the observable  $P_t$  can be used to distinguish a pseudoscalar from a scalar Higgs, the use of  $P_t$  alone does not allow for an accurate extraction of  $a$  and  $b$ , unless the parameter range has been constrained elsewhere before.

### 2.3 Ratios of cross sections

Scalar and pseudoscalar Higgs production differ by their threshold behaviour. A simple method to test this different behaviour is the measurement of the total cross section at two different c.m. energies. These should both be below  $\sim 800$  GeV, so that they lie within the region of rising  $\sigma$ , and the number of events should not be too small. As c.m. energies we therefore chose  $\sqrt{s_1} = 800$  GeV and  $\sqrt{s_2} = 600$  GeV and investigated the ratio

$$R = \frac{\sigma(\sqrt{s_1})}{\sigma(\sqrt{s_2})}. \quad (17)$$

The advantage of investigating ratios of cross sections is that the effect an overall model-dependent normalization of the top quark Yukawa coupling and some systematic errors in the measurement can be avoided. We found, however, that the results for  $\Delta a^\pm$  and  $\Delta b^\pm$  show the same behaviour as for the observable  $P_t$ . The ratio  $R$  is a good observable to distinguish a purely CP-odd from a CP-even Higgs boson in case of a CP-conserving Higgs sector, or to distinguish a CP-mixed Higgs state with a large CP-odd contribution from a CP-even Higgs. It is difficult, however, to extract the absolute values of  $a$  and  $b$  in a model-independent approach over the whole considered  $a - b$  parameter range. In the following we will therefore not use  $R$ , but instead  $P_t$  (together with the total cross section and the up-down asymmetry) to determine the CP quantum numbers. It

may be possible to measure the ratio  $R$  more accurately, but this requires running at two different collider energies, whereas for the measurement of  $P_t$ , while more complex, running at a single energy suffices.

## 2.4 The CP-violating up-down asymmetry

Contrary to the total cross section and the top polarisation asymmetry the up-down asymmetry  $A_\phi$  of the antitop with respect to the top-electron plane is an observable which is sensitive to CP violation. Defining by  $q_{a,b}$  the four-momenta of the incoming  $e^-, e^+$  and by  $p_{1,2}$  the four-momenta of the top, antitop, respectively, the angle  $\phi$  between the antitop direction and the top-electron plane is given by

$$\sin \phi = \frac{\vec{p}_2(\vec{q}_a \times \vec{p}_1)}{|\vec{p}_2||\vec{q}_a \times \vec{p}_1|} \sim \epsilon^{p_1 p_2 q_a q_b}, \quad (18)$$

with the totally antisymmetric Levi-Civita tensor  $\epsilon$ . The up-down asymmetry of the  $t\bar{t}\Phi$  cross section  $\sigma$  is defined as

$$A_\phi = \frac{\sigma(\text{up}) - \sigma(\text{down})}{\sigma(\text{up}) + \sigma(\text{down})}, \quad (19)$$

where 'up' ('down') denotes the value of the cross section if the integration over  $\phi$  is performed for  $\phi \in [0, \pi)$  ( $\phi \in [\pi, 2\pi)$ ). It turns out that  $A_\phi$  is given by the interference of the diagram where the Higgs is radiated from the top-quark with the diagram where the Higgs is radiated from the  $Z$  boson [41]. The asymmetry can be cast into the form

$$A_\phi = \frac{\sigma_{asbc}}{\sigma}, \quad (20)$$

with the numerator of Eq. (20) denoting the asymmetric interference term proportional to  $bc$ , which can be derived from the differential cross section given in Eq. (29) of the Appendix. The denominator is given by the total cross section  $\sigma = \sigma(\text{up}) + \sigma(\text{down})$ . A non-vanishing  $A_\phi$  is an unambiguous indicator of CP violation. As it is proportional to  $b$ , the  $t\bar{t}\Phi$  coupling must contain a CP-odd part. If, however, the Higgs sector is CP-conserving and a purely CP-odd Higgs boson is radiated from the top line, the coupling to the  $Z$  boson must vanish at tree-level, *i.e.*  $c = 0$ , so that in the CP-conserving case  $A_\phi = 0$ . The contour lines of  $A_\phi$  are shown in Fig. 9 in the  $a - b$  parameter plane for  $M_\Phi = 120$  GeV and  $\sqrt{s} = 800$  GeV. The incoming  $e^\pm$  beams are unpolarised. As we put  $c = -a$ , the up-down asymmetry depends in the numerator linearly on  $a$  and  $b$ . In the denominator it depends via the total cross section quadratically on  $a$  and  $b$ . The asymmetry is shown for positive values  $a$  and  $b$ . It can be inferred for the negative values from its asymmetric behaviour with respect to a sign change of  $a$  or  $b$ . We found that the polarisation of the initial beams does not help to increase  $A_\phi$ . The polarisation of the  $e^\pm$  beams contributes differently to the various terms entering the total cross section, which is in the denominator of  $A_\phi$ , and to the interference term  $\sim bc$  in the numerator of  $A_\phi$ . This results in a small net effect on  $A_\phi$  of the initial beam polarisation. This can also be inferred from the formulae of the various terms for polarised  $e^\pm$  beams which can be derived by using the formulae given in the Appendix. For higher c.m. energies the asymmetry is larger, as the cross section in the denominator decreases faster with rising  $\sqrt{s}$  as the numerator. However, the total number of events will decrease for the same reason, which can

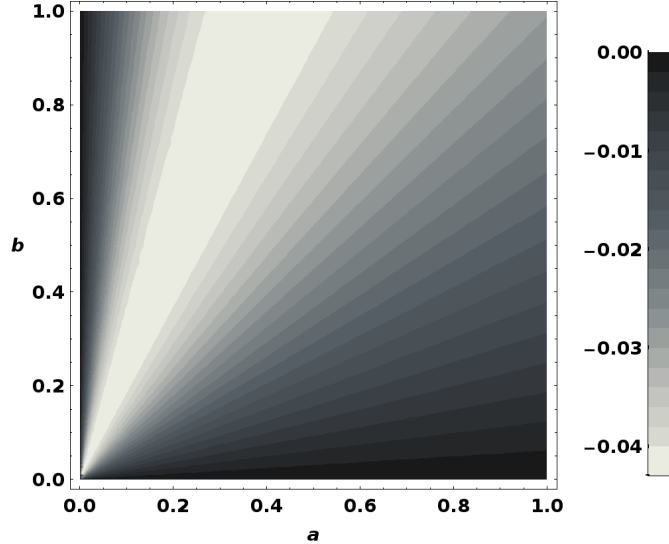


Figure 9: Contour plot of the up-down asymmetry  $A_\phi$  in the  $a - b$  parameter plane for  $M_H = 120$  GeV and  $\sqrt{s} = 800$  GeV. The  $e^\pm$  beams are unpolarised. The grey code indicates the value of  $A_\phi$ .

be balanced by a higher luminosity.

The errors on  $a$ ,  $b$  have been extracted in the same way as before with  $\Delta O(a_0, b_0)$  of Eq. (6) given by

$$\Delta O(a_0, b_0) = \Delta A_\phi = \frac{1}{\sqrt{\sigma \mathcal{L}}} \sqrt{1 - A_\phi^2}. \quad (21)$$

The errors extracted solely from  $A_\phi$  turn out to be larger than the absolute values of  $a$ ,  $b$ . This is the result of an interplay of a too small variation of  $A_\phi$  with  $a$  and/or  $b$  and too large errors  $\Delta A_\phi$ .

We conclude this subsection by showing in Fig. 10 the up-down asymmetry in case we impose  $a^2 = 1 - b^2$ . Being proportional to  $b$  it vanishes for  $b = 0$ . As it is also proportional to  $c$ , at  $b = 1$ , where  $a = 0$ , it vanishes due to our choice  $c = -a$ . As can be inferred from the figure, switching the polarisation from  $P_{e^-} = -0.8, P_{e^+} = 0.6$  to  $P_{e^-} = 0.8, P_{e^+} = -0.6$  slightly increases  $A_\phi$ . In this case, however, the cross section is not increased by about a factor of 2 any more as in the case of our original choice of  $P_{e^\pm}$ , but is decreased by about 10%.

## 2.5 The combined sensitivity

As has been discussed in the previous subsections the total cross section is a good observable to determine  $a$ , whereas less good for the measurement of  $b$ . The top polarisation asymmetry, on the other hand, can only be used to distinguish a CP-odd from a CP-even Higgs boson. The up-down asymmetry  $A_\phi$  tests CP-mixing, but the errors on  $a$  and  $b$  are too large to be useful for a determination of  $a$ ,  $b$ . The accuracy on  $a$  ( $b$ ) will substantially improve, however, if the parameter  $b$  ( $a$ ) has been extracted beforehand from some other measurement. We therefore combine all three observables  $O_i$  ( $i = 1, 2, 3$ ) given by  $\sigma$ ,  $P_t$  and  $A_\phi$  to derive new sensitivity areas for  $a$  and  $b$  by

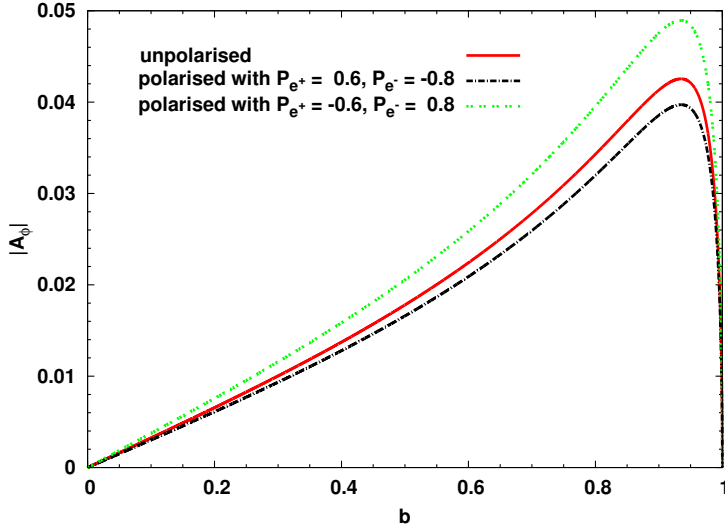


Figure 10: The absolute value of the up-down asymmetry  $A_\phi$  as function of  $b$  with  $a^2 + b^2 = 1$ , for unpolarised beams (red/full), polarised beams with  $P_{e^-} = -0.8, P_{e^+} = 0.6$  (black/dash-dotted) and polarised beams with  $P_{e^-} = 0.8, P_{e^+} = -0.6$  (green/dotted).

performing a  $\chi^2$  test, with  $\chi^2$  defined as

$$\chi^2 = \sum_{i=1,2,3} \frac{(O_i(a, b) - O_i(a_0, b_0))^2}{(\Delta O_i(a_0, b_0))^2}. \quad (22)$$

The errors  $\Delta a^\pm, \Delta b^\pm$  are again determined by the maximal extensions of the insensitive areas and are shown at  $1\sigma$  confidence level in Fig. 11 for unpolarised and in Fig. 12 for polarised beams with  $\sqrt{s} = 800$  GeV and  $\int \mathcal{L} = 500$  fb $^{-1}$ .

In case of unpolarised beams the plots essentially reproduce the errors on  $a$  and  $b$  extracted from the total cross section alone. This was expected since it is the most sensitive observable and  $P_t$  and  $A_\phi$  do not help to improve the errors in this case. If the initial beams are polarised, however, the errors on  $a$  are remarkably reduced. This is due to the mutual interplay between  $\sigma$  and  $P_t$  in constraining the parameter ranges of  $a$  and  $b$ . The polarisation is necessary in order to increase the cross section and  $P_t$ . For  $P_t$  this also leads to a smaller statistical fluctuation  $\Delta P_t \sim 1/\sqrt{\sigma \mathcal{L}}$ . As for  $b$ , polarisation slightly helps to decrease the error for  $|b| \gtrsim 0.5$ . The observable  $A_\phi$  does not have any effect on the reduction of the errors at  $\sqrt{s} = 800$  GeV.

At high c.m. energies of  $\sqrt{s} = 3 - 5$  TeV as realized in the CLIC design [63] the total cross section, which scales with the energy, is smaller. On the other hand this will be balanced by higher integrated luminosities of  $\int \mathcal{L} = 3 - 5$  ab $^{-1}$ , so that the signal rate approximately remains the same. The top polarisation asymmetry does not change a lot compared to 800 GeV c.m. energy, as can be extrapolated from Fig. 7, which shows  $P_t$  as a function of  $\sqrt{s}$ . The statistical fluctuation  $\Delta P_t$ , which is inversely proportional to the signal rate, almost does not change either. The up-down asymmetry, however, gets larger with rising  $\sqrt{s}$ . Therefore at high energies in the multi-TeV regime all three observables contribute significantly to  $\chi^2$ . Their mutual interplay results in remarkably small errors on  $a$  less than about 0.2 in large parts of the parameter space. This can be inferred from Fig. 13, which shows for  $\sqrt{s} = 3$  TeV and  $\mathcal{L} = 3$  ab $^{-1}$  the errors on  $a$  and  $b$  at  $1\sigma$  confidence

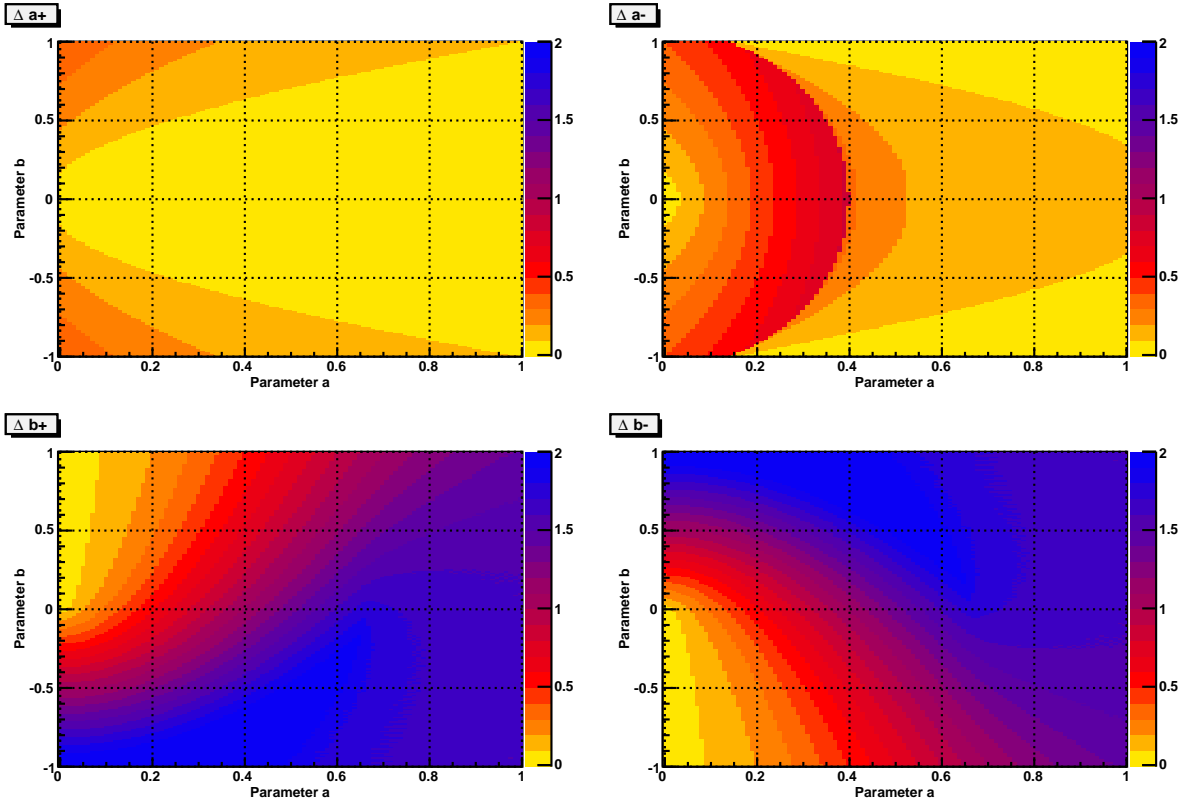


Figure 11: Errors  $\Delta a^+$  (upper left) and  $\Delta a^-$  (upper right) on  $a$  as well as  $\Delta b^+$  (lower left) and  $\Delta b^-$  (lower right) on  $b$ , by combining all 3 observables  $\sigma, P_t, A_\phi$ , at  $1\sigma$  confidence level for  $M_\Phi = 120$  GeV and  $\sqrt{s} = 800$  GeV with  $\mathcal{L} = 500$  fb $^{-1}$ . The  $e^\pm$  beams are unpolarised. The colour code indicates the magnitude of the respective error.

level extracted from the combination of all three observables for polarised beams. It turns out that  $P_t$  and  $A_\phi$  contribute to the reduction of the error in complementary areas of the  $a - b$  parameter plane. As for  $b$ , the error is  $\lesssim 0.3$  except for low values of  $a$  and  $b$  values around  $\sim \pm 0.2$ , where it gets worse.

### 3 Radiation of a spin 1 particle

In this section we investigate the question to what extent the spin of the particle produced in association with a  $t\bar{t}$  pair affects the total cross section and the polarisation asymmetry. The motivation is two-fold. On the one hand  $t\bar{t}Z$  production contributes a large part to the irreducible SM background of associated Higgs production, so that a distinction of these two processes for the identification of the signal process is necessary [53]. On the other hand numerous models of New Physics predict the existence of additional neutral particles  $Z'$  with spin  $J = 1$ . In the following the associated production of such a particle will be investigated without referring to a specific model.<sup>3</sup> This particle is only demanded to couple to top quarks but not to  $e^\pm$ , like the

<sup>3</sup>See Ref. [64] for associated SM  $Z$  boson production with anomalous couplings.



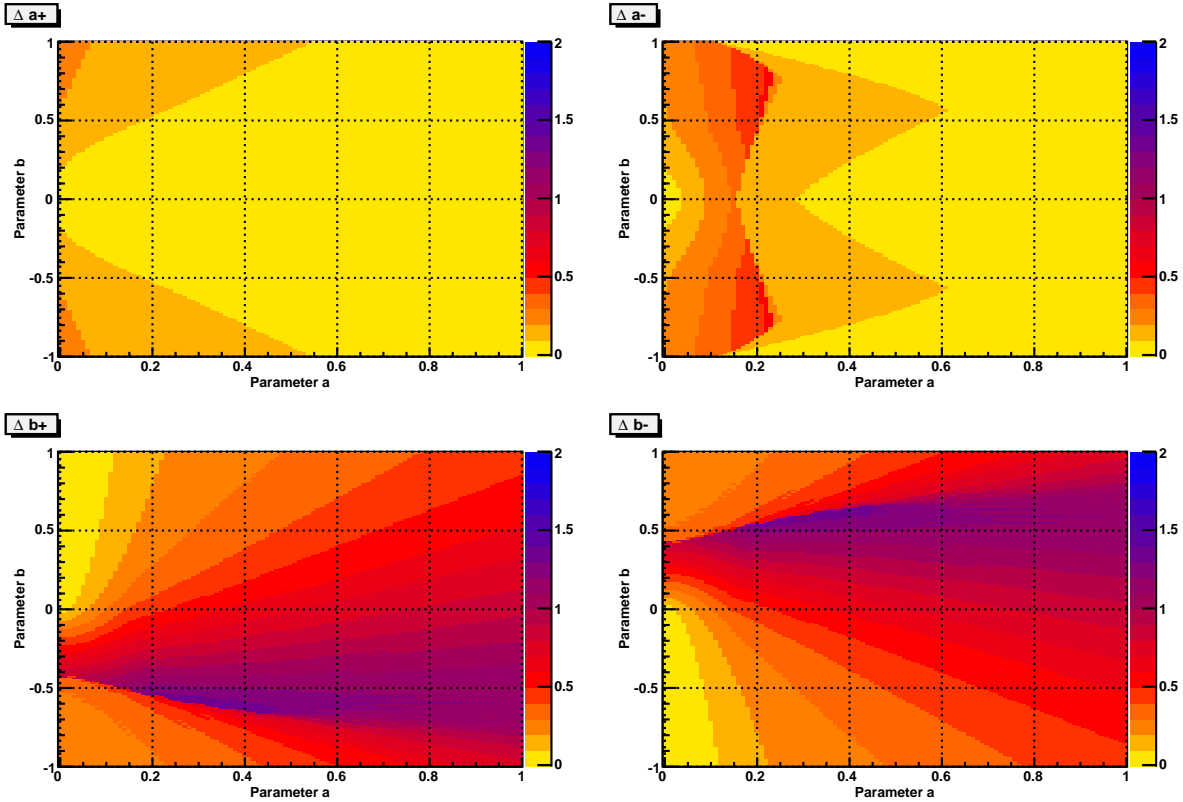


Figure 12: Same as Fig. 11, but for polarised  $e^\pm$  beams.

SM Higgs boson.<sup>4</sup> The description of the  $t\bar{t}Z'$  coupling in an effective model-independent ansatz demanding Lorentz invariance and hermiticity and including terms of up to dimension 5 depends on ten parameters [65]. In a first approach we do not take into account anomalous vector couplings to  $t\bar{t}$  of dimension higher than 4. This will be left to a future publication. The  $t\bar{t}Z'$  coupling is hence given by

$$C_{t\bar{t}Z'} = -ie\gamma_\mu(g_V - g_A\gamma_5), \quad (23)$$

with the vector and axial-vector couplings  $g_V$  and  $g_A$  chosen to be of  $\mathcal{O}(1)$ .

Assuming a particle with mass of 120 GeV has been produced at an  $e^+e^-$  collider in association with a top-quark pair, it is investigated if the cross section and its energy dependence as well as  $P_t$  allow for the distinction of a SM Higgs  $H^0$  (and hence a spin 0 particle) from a spin 1 particle. We therefore consider  $e^+e^- \rightarrow t\bar{t}Z'$  production of a  $Z'$  with mass  $M_{Z'} = M_{H^0} = 120$  GeV. The cross section is assumed to have the same magnitude as expected for the production of a SM Higgs with this mass value and a c.m. energy of 800 GeV, within an error of 10%. This is the error on SM Higgs production to be expected for these parameter values at an ILC. This condition leads to a range  $\mathcal{P}$  of values  $g_V$  and  $g_A$ , *i.e.*

$$g_V, g_A \in \mathcal{P} \iff \sigma_{t\bar{t}Z'}(g_V, g_A) = \sigma_{t\bar{t}H^0} \pm 10\%. \quad (24)$$

<sup>4</sup>A non-vanishing coupling  $eeZ'$  would have been excluded by the LEP experiments for the masses we study.

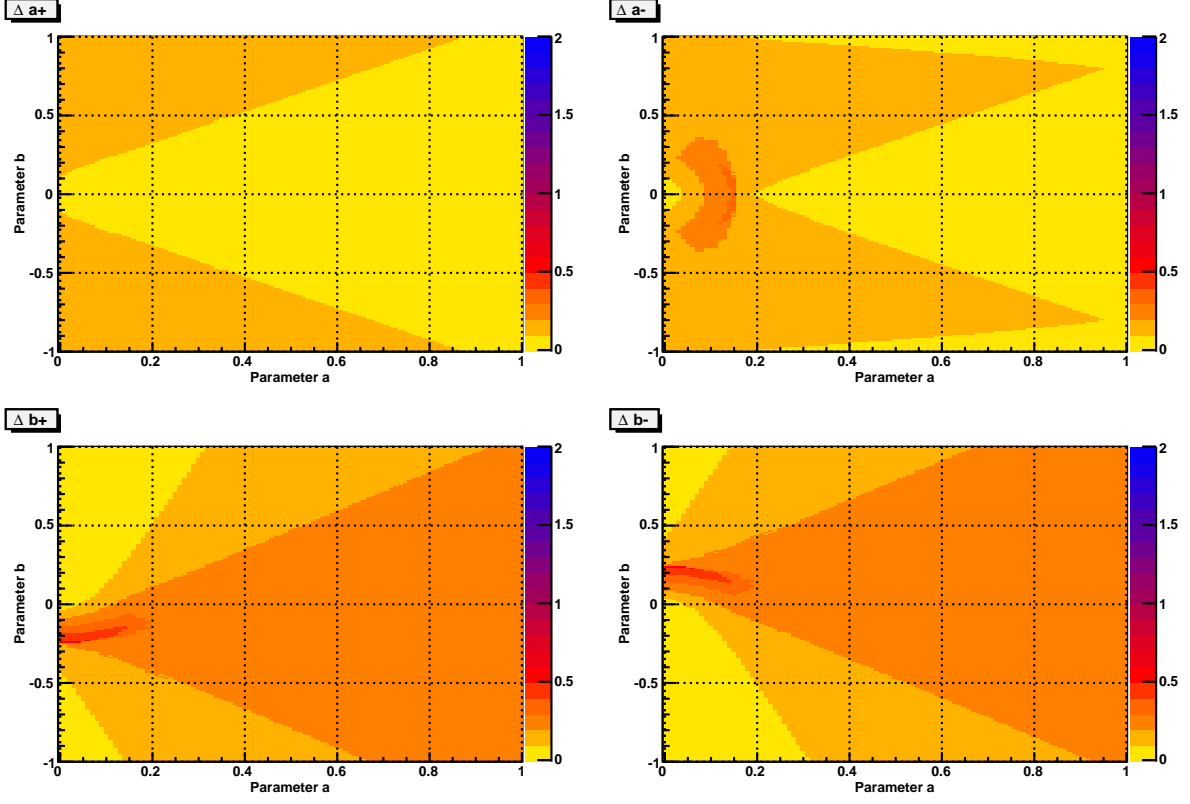


Figure 13: Errors  $\Delta a^+$  (upper left) and  $\Delta a^-$  (upper right) on  $a$  as well as  $\Delta b^+$  (lower left) and  $\Delta b^-$  (lower right) on  $b$ , by combining all 3 observables  $\sigma, P_t, A_\phi$ , at  $1\sigma$  confidence level for  $M_\Phi = 120$  GeV and  $\sqrt{s} = 3$  TeV with  $\mathcal{L} = 3$  ab $^{-1}$ . The  $e^\pm$  beams are polarised. The colour code indicates the magnitude of the respective error.

For these values, the top polarisation asymmetry is calculated and compared to  $P_t(t\bar{t}H^0) = 0.11$ . Fig. 14 (upper left) shows the values of  $P_t(t\bar{t}Z')$  for the range of values  $\mathcal{P}$ . The white strips in the coloured area appear where  $P_t(t\bar{t}Z')$  differs from  $P_t(t\bar{t}H^0)$  by less than  $5\sigma$ . These regions are small. We conclude that for a particle produced in association with a top quark pair with the same rate within the experimental error as expected from  $t\bar{t}H^0$  production, the top polarisation asymmetry can be exploited to distinguish a spin 1 state from a spin 0 state if neither  $g_V$  nor  $g_A$  is close to 0.

Moreover, the ratio of cross sections at different c.m. energies can be exploited. This is shown in Figs. 14 upper right, lower left and lower right. The ratio of the  $t\bar{t}Z'$  cross section at two different collider energies for three c.m. energy combinations, respectively, is plotted for the parameter range  $\mathcal{P}$  as defined above. All three ratio combinations are larger than the corresponding SM values and differ from them by more than  $5\sigma$ . The SM values are

$$\begin{aligned}
 \frac{\sigma_{H^0 t\bar{t}}(1000 \text{ GeV})}{\sigma_{H^0 t\bar{t}}(800 \text{ GeV})} &= 0.85 & \frac{\sigma_{H^0 t\bar{t}}(1300 \text{ GeV})}{\sigma_{H^0 t\bar{t}}(800 \text{ GeV})} &= 0.61 \\
 \frac{\sigma_{H^0 t\bar{t}}(1300 \text{ GeV})}{\sigma_{H^0 t\bar{t}}(1000 \text{ GeV})} &= 0.72 . & & 
 \end{aligned} \tag{25}$$

The SM ratios are very different from the  $t\bar{t}Z'$  production ratios since the maximum of the SM

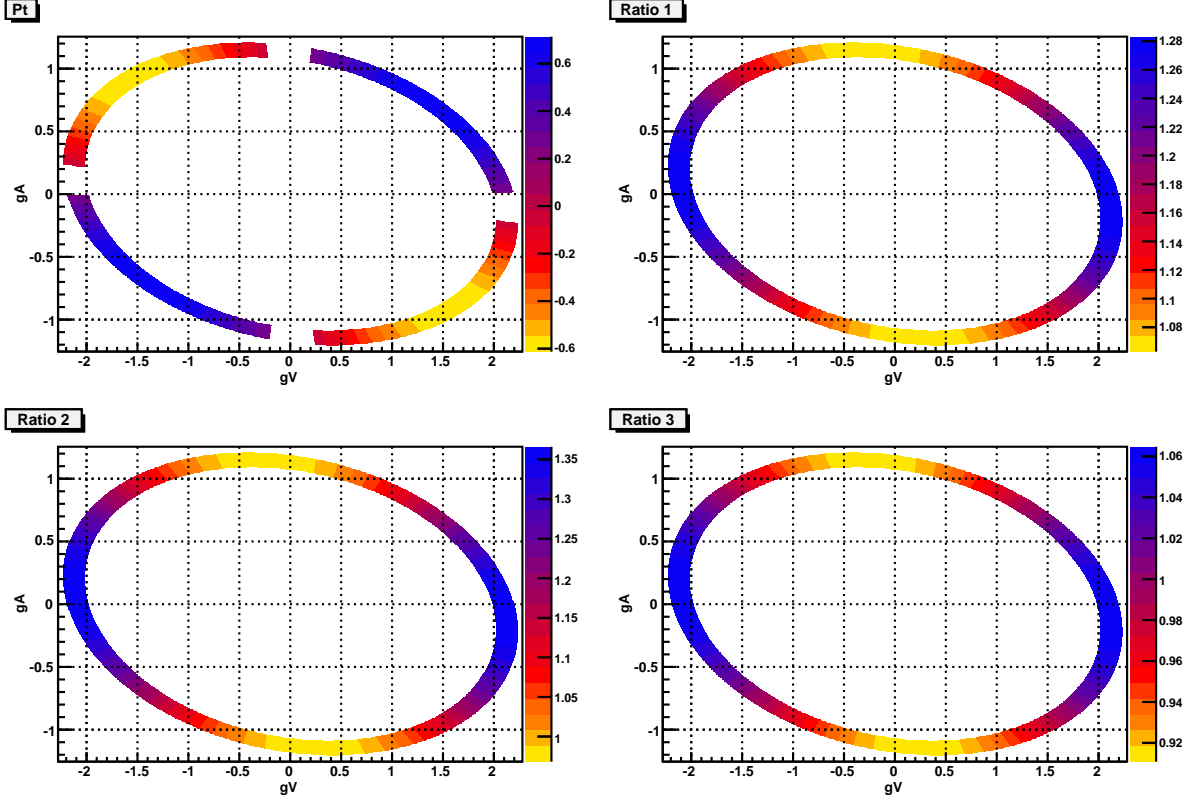


Figure 14: The  $P_t$  contours for  $t\bar{t}Z'$  production with  $M_{Z'} = 120$  GeV and  $\sqrt{s} = 800$  GeV (upper left). The contours for the ratio of the cross sections at different c.m. energies are shown in the upper right plot for  $\sigma(1000 \text{ GeV})/\sigma(800 \text{ GeV})$ , the lower left plot for  $\sigma(1300 \text{ GeV})/\sigma(800 \text{ GeV})$  and the lower right plot for  $\sigma(1300 \text{ GeV})/\sigma(1000 \text{ GeV})$ . The colour code indicates the magnitude of  $P_t$  and of the ratios, respectively. The couplings  $g_A$  and  $g_V$  have been chosen as described in the text.

cross section occurs at  $\sim 750$  GeV and hence all considered ratios in case of the SM Higgs are less than 1. For  $t\bar{t}Z'$  production the maximum lies at 1000 GeV or higher, depending on the values of  $g_V$ ,  $g_A$ . Although these results of course depend on the mass of the particle radiated from the top quark pair and on the considered energies, they show that the top polarisation asymmetry and/or ratios of cross sections are sensitive to the spin value of the particle produced in association with  $t\bar{t}$ .

This statement is confirmed by the plots presented in Figs. 15 and 16. Figure 15 shows the total cross section  $\sigma(t\bar{t}Z')$  compared to the cross section of scalar Higgs production in association with a top quark pair,  $\sigma(t\bar{t}H)$ . The  $H$  and  $Z'$  masses have been chosen equal,  $M_{Z'} = M_H = 120$  GeV. For the Higgs coupling to the top quark pair the maximum coupling strength  $a = 1$  has been adopted. The couplings  $g_V$  and  $g_A$  have been chosen within a parameter range  $\mathcal{P}'$  such that the maxima of the two cross sections in comparison are the same,

$$g_V, g_A \in \mathcal{P}' \iff \sigma_{t\bar{t}Z'}^{\max}(g_V, g_A) = \sigma_{t\bar{t}H}^{\max}. \quad (26)$$

Three cases are studied, where either  $g_V$  or  $g_A$  are non-zero and where both  $g_V$  and  $g_A$  are non-zero.

Figure 16 shows the comparison of  $\sigma(t\bar{t}Z')$  with the associated production of a pseudoscalar  $A$  with a top quark pair,  $\sigma(t\bar{t}A)$ , for  $M_{Z'} = M_A = 120$  GeV. For the CP-odd coupling parameter to the top quarks  $b = 1$  has been assumed. The coupling parameters  $g_V, g_A$  have been chosen as before within a parameter range  $\mathcal{P}''$  such that the maximum values of the cross sections are the same,

$$g_V, g_A \in \mathcal{P}'' \iff \sigma_{t\bar{t}Z'}^{\max}(g_V, g_A) = \sigma_{t\bar{t}A}^{\max}, \quad (27)$$

and once again three types of coupling combinations  $g_V$  and  $g_A$  are investigated. As can be inferred from the figures, the curves for spin 1 production and CP-odd Higgs production are very similar both in the threshold rise and in the continuum. This is to be contrasted with the comparison of the curves for spin 1 production and CP-even Higgs production. The threshold rise is not so much different. But in the continuum they clearly differ. This reproduces the difference in the ratios of cross sections observed above.

## 4 Summary

Once a Higgs boson has been discovered at the LHC, its CP properties have to be determined. Should the Higgs boson not be CP-even but CP-odd or a CP-mixed state, then the top sector represents an ideal working ground to test its CP properties, since the various possible CP-parts of the Higgs boson couple democratically to the top quarks. This is in contrast to the Higgs coupling to gauge bosons which projects out the CP-even part of the coupling and has only a small admixture of CP-odd parts from loop diagrams. In this paper, we investigated the production of a spin 0 state with arbitrary model-independent CP properties in association with a top quark pair at a future  $e^+e^-$  linear collider. The CP properties of the Higgs coupling to the top quarks have been parametrized in a model-independent way by a parameter  $a$  for a CP-even Higgs, by a parameter  $b$  for a CP-odd Higgs and by simultaneously non-vanishing  $a$  and  $b$  for a CP-mixed state. These parameters can be determined by a measurement of the total cross section, the polarisation asymmetry of the top quark and the up-down asymmetry of the antitop quark with respect to the top-electron plane. The former two observables are CP-even and can be exploited to distinguish a CP-even from a CP-odd Higgs boson. Since the up-down asymmetry  $A_\phi$  is CP-odd, it can be exploited directly and unambiguously to test CP violation.

The sensitivities to  $a$  and  $b$  have been studied in each observable separately before investigating the combination of all three observables. We found that the total cross section is most sensitive to  $a$  and to some extent to  $b$ . The observables  $P_t$  and  $A_\phi$  do not exhibit much sensitivity to  $a$  and  $b$ , although polarisation of the initial  $e^\pm$  beams slightly improves the sensitivity in case of  $P_t$ . The combination of all three observables, however, remarkably reduces the error on  $a$  for polarised  $e^\pm$  beams. At 800 GeV c.m. energy this is due to the mutual interplay of  $\sigma$  and  $P_t$  in constraining the parameter range of  $a$  and  $b$ . At multi-TeV energies  $A_\phi$  is larger, and it is now the interplay of all three observables which further reduces the error.

We also investigated to what extent the radiation of an arbitrary spin 1 particle from the top quark pair, which like the Higgs boson does not couple to  $e^\pm$ , can be distinguished from a spin 0 state with the same mass. It turns out that the top polarisation asymmetry and ratios of cross sections at different collider energies represent good observables to tell a spin 0 from a spin 1 state.

In summary, associated Higgs production with a  $t\bar{t}$  pair at a future  $e^+e^-$  collider allows for

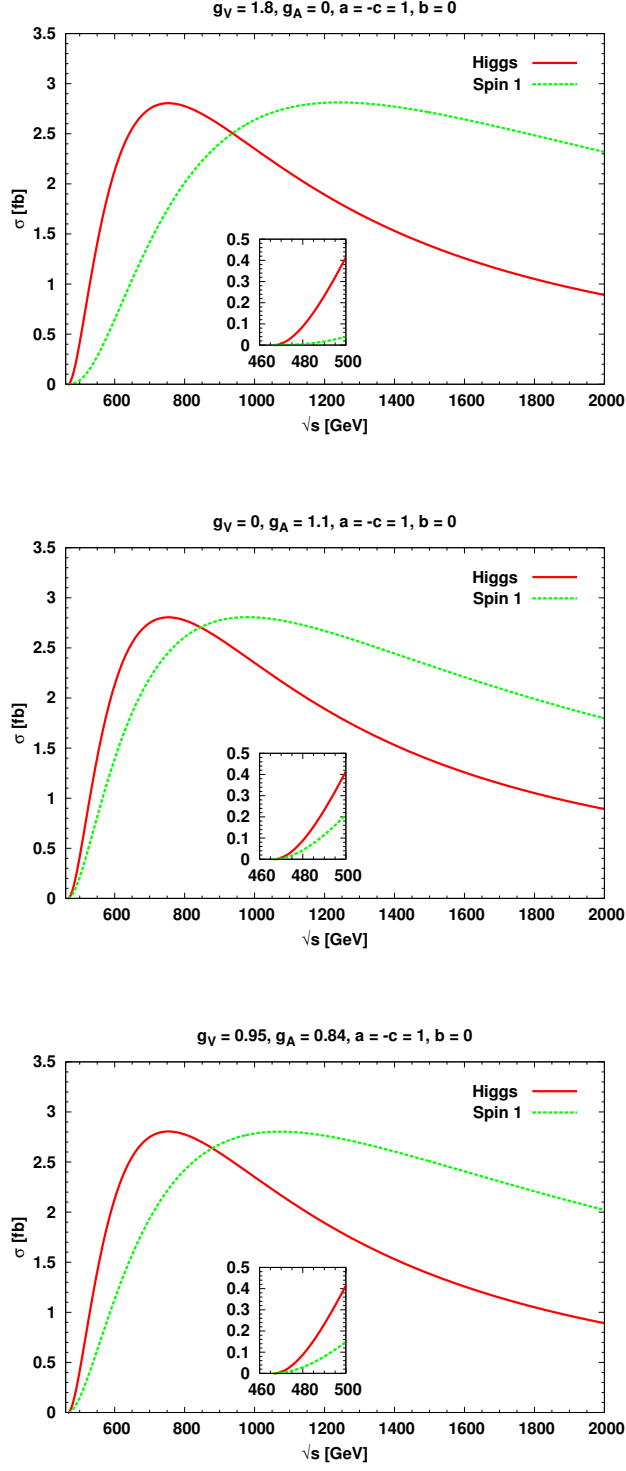


Figure 15: Total cross section  $\sigma(t\bar{t}H)$  (red/full) compared to  $\sigma(t\bar{t}Z')$  (green/dashed) as function of the c.m. energy for  $M_{Z'} = M_H = 120$  GeV. The parameters  $g_V \neq 0$  (upper),  $g_A \neq 0$  (middle) and  $g_V, g_A \neq 0$  (lower) have been chosen such that the maximum values of the cross sections are the same.

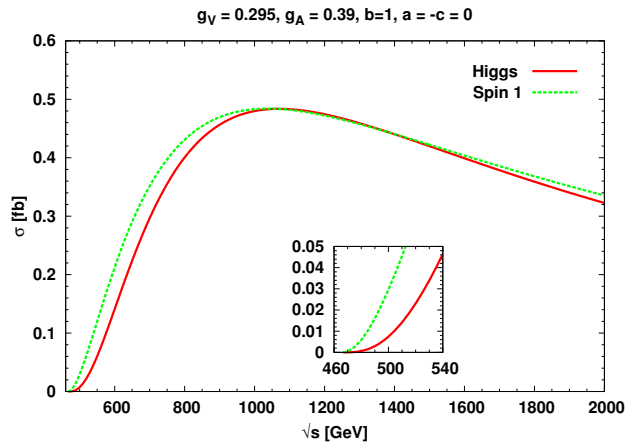
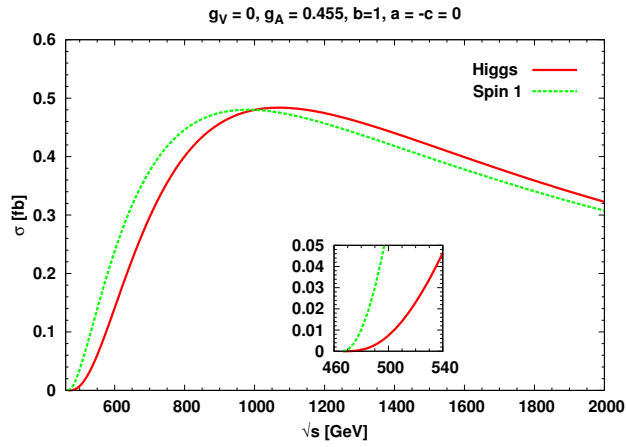
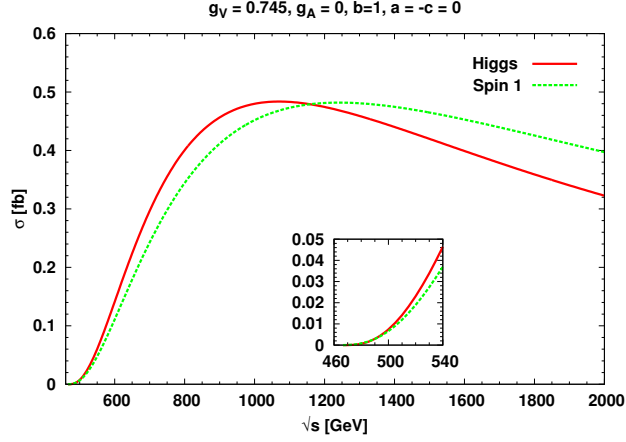


Figure 16: Total cross section  $\sigma(t\bar{t}A)$  (red/full) compared to  $\sigma(t\bar{t}Z')$  (green/dashed) as function of the c.m. energy for  $M_{Z'} = M_A = 120$  GeV. The parameters  $g_V \neq 0$  (upper),  $g_A \neq 0$  (middle) and  $g_V, g_A \neq 0$  (lower) have been chosen such that the maximum values of the cross sections are the same.

the determination of the spin and CP properties of the Higgs boson in a model-independent way. Combining the total cross section and its energy dependence, the top polarisation asymmetry and the up-down asymmetry considerably helps to reduce the errors on the coupling parameters of the Higgs Yukawa coupling which reveal the CP nature of the Higgs boson.

## Appendix

### Cross sections for initial beam polarisation

The cross sections  $\sigma_0$  and  $\sigma_1$  as defined in Eq. (9) get modified for initial beam polarisation. The polarisation acts differently on the contributions to the cross sections from the various diagrams. The changes can be summarized by replacing the coupling factors in the cross sections. Denoting by  $P_{e^-}$  and  $P_{e^+}$  the degree of longitudinal polarisation of the electron and positron, respectively, the changes to be applied for the couplings appearing in  $\sigma = 2\sigma_0$  Eq. (4) and  $\sigma_1$  Eq. (12) are

$$\begin{aligned} Q_e^2 Q_t^2 &\rightarrow Q_e^2 Q_t^2 (1 - P_{e^+} P_{e^-}) \\ 2Q_e Q_t v_e &\rightarrow 2Q_e Q_t [v_e (1 - P_{e^+} P_{e^-}) + a_e (P_{e^+} - P_{e^-})] \\ (v_e^2 + a_e^2) &\rightarrow [(v_e^2 + a_e^2) (1 - P_{e^+} P_{e^-}) + 2v_e a_e (P_{e^+} - P_{e^-})] . \end{aligned} \quad (28)$$

The up-down asymmetry originates from the interference term between the diagrams where the Higgs is radiated from the top line and the one where the Higgs is radiated from the  $Z$  boson. The denominator of  $A_\phi$  is simply given by the total cross section *cf.* Eq. (20). The differential cross section for the interference term  $\sim bc$  reads in terms of the scaled Mandelstam variables  $S_1, S_2, T_1, T_2$

$$\begin{aligned} \frac{d\sigma_{bc}}{dS_1 dS_2 dT_1 dT_2} &= \frac{3\alpha^2}{8\pi^2 s^3} \frac{bc g_{ttHGZZH} \sqrt{h_t/s}}{h_Z (S_1 - h_Z) (S_2 - h_t) (-1 + S_1 + S_2 - h_t - h_\Phi)} \times \\ &\left\{ \frac{Q_e Q_t a_t a_e}{(h_Z - 1)} D_1^\Phi + \frac{2a_e v_e a_t v_t}{(h_Z - 1)^2} D_2^\Phi + \frac{a_t^2 (a_e^2 + v_e^2)}{(h_Z - 1)^2} D_3^\Phi \right\} \epsilon^{p_1 p_2 q_a q_b} , \end{aligned} \quad (29)$$

with  $h_X = m_X^2/s$  and the form factors given by

$$D_1^\Phi = (h_\Phi + 1 - S_1)(h_\Phi - 2h_Z - 1 + S_1) \quad (30)$$

$$D_2^\Phi = (1 - S_1)^2 - h_\Phi^2 \quad (31)$$

$$D_3^\Phi = (-h_\Phi - 2h_t - 1 + S_1 + 2S_2)(h_\Phi - 1 + S_1 - 2T_2) . \quad (32)$$

The scaled Mandelstam variables in terms of the reduced energies  $x_1, x_2$ , the azimuthal angle  $\chi$  of the antitop, the polar angle  $\theta$  of the top quark, the angle  $\theta_{12}$  between top and antitop and the velocities  $\beta_{1,2} = \sqrt{1 - 4h_t/x_{1,2}^2}$  read

$$S_1 = 1 - h_\Phi - x_3 \quad (33)$$

$$S_2 = 1 + h_t - x_1 \quad (34)$$

$$T_1 = h_t - \frac{1}{2} x_1 (1 - \beta_1 \cos \theta) \quad (35)$$

$$T_2 = h_\Phi - \frac{1}{2} x_1 [x_3 - \sin \theta \sin \theta_{12} \cos \chi x_2 \beta_2 - \cos \theta (x_1 \beta_1 + x_2 \beta_2 \cos \theta_{12})] . \quad (36)$$

In case of polarised  $e^\pm$  beams, the following replacements for the coupling factors have to be made

$$\begin{aligned}
Q_e Q_t a_e &\rightarrow Q_e Q_t [a_e(1 - P_{e^+} P_{e^-}) + v_e(P_{e^+} - P_{e^-})] \\
2a_e v_e &\rightarrow [2v_e a_e(1 - P_{e^+} P_{e^-}) + (a_e^2 + v_e^2)(P_{e^+} - P_{e^-})] \\
(a_e^2 + v_e^2) &\rightarrow [(a_e^2 + v_e^2)(1 - P_{e^+} P_{e^-}) + 2a_e v_e(P_{e^+} - P_{e^-})].
\end{aligned} \tag{37}$$

## Acknowledgments

RG and SDR wish to acknowledge support from the Department of Science and Technology, India under the J.C. Bose Fellowship scheme under grant nos. SR/S2/JCB-64/2007 and SR/S2/JCB-42/2009, respectively. CH and MM acknowledge support from the Deutsche Forschungsgemeinschaft via the Sonderforschungsbereich/Transregio SFB/TR-9 Computational Particle Physics.

## References

- [1] J. Goldstone, A. Salam and S. Weinberg, Phys. Rev. **127** (1962) 965; S. Weinberg, Phys. Rev. Lett. **19** (1967) 1264; S.L. Glashow, S. Weinberg, Phys. Rev. Lett. **20** (1968) 224; A. Salam, Proceedings Of The Nobel Symposium, Stockholm 1968, ed. N. Svartholm.
- [2] P.W. Higgs, Phys. Lett. **12** (1964) 132 and Phys. Rev. **145** (1966) 1156; F. Englert and R. Brout, Phys. Rev. Lett. **13** (1964) 321; P. W. Higgs, Phys. Rev. Lett. **13** (1964) 508; G.S. Guralnik, C.R. Hagen and T.W. Kibble, Phys. Rev. Lett. **13** (1964) 585.
- [3] For reviews see: J.F. Gunion, H.E. Haber, G. Kane and S. Dawson, “*The Higgs Hunter’s Guide*”, Addison-Wesley, 1990; R. M. Godbole, [hep-ph/0205114]; A. Djouadi, Phys. Rept. **457** (2008) 216 [hep-ph/0503172]; M. Gomez-Bock, M. Mondragon, M. Mühlleitner, R. Noriega-Papaqui, I. Pedraza, M. Spira and P. M. Zerwas, J. Phys. Conf. Ser. **18** (2005) 74 [arXiv:hep-ph/0509077]; M. Gomez-Bock, M. Mondragon, M. Mühlleitner, M. Spira and P. M. Zerwas, [arXiv:0712.2419 [hep-ph]]; A. Djouadi, R. M. Godbole, in “*Physics at the Large Hadron Collider*”, Ed. A. Datta, B. Mukhopadhyaya and A. Raychaudhuri, Springer (India), New Delhi, pp. 47-74 [arXiv:0901.2030 [hep-ph]].
- [4] ATLAS Collaboration, Technical Design Report, CERN-LHCC-14 and CERN-LHCC-15; CMS Collaboration, Technical Design Report, CMS-LHCC-2006-21.
- [5] E. Accomando *et al.* [ECFA/DESY LC Physics Working Group Collaboration], Phys. Rept. **299** (1998) 1 [hep-ph/9705442]; J. A. Aguilar-Saavedra *et al.* [ECFA/DESY LC Physics Working Group Collaboration], [hep-ph/0106315]; T. Abe *et al.* [American Linear Collider Working Group Collaboration], [hep-ex/0106055-58]; K. Abe *et al.* [ACFA Linear Collider Working Group Collaboration], [hep-ph/0109166]; G. Aarons *et al.* [ILC Collaboration], [arXiv:0709.1893 [hep-ph]].
- [6] G. Weiglein *et al.*, Phys. Rept. **426** (2006) 47.
- [7] F. Boudjema, E. Chopin, Z. Phys. **C73** (1996) 85 [hep-ph/9507396]; A. Djouadi, W. Kilian, M. Mühlleitner *et al.*, Eur. Phys. J. **C10** (1999) 27 [hep-ph/9903229]; A. Djouadi, W. Kilian, M. Mühlleitner and P. M. Zerwas, Eur. Phys. J. **C 10** (1999) 45 [hep-ph/9904287]; A. Djouadi,



- W. Kilian, M. Mühlleitner and P. M. Zerwas, [hep-ph/0001169]; M. M. Mühlleitner, [hep-ph/0008127]; E. Asakawa, D. Harada, S. Kanemura *et al.*, Phys. Rev. **D82** (2010) 115002 [arXiv:1009.4670 [hep-ph]].
- [8] D.V. Volkov and V.P. Alkulov, Phys. Lett. **B46** (1973) 109; J. Wess and B. Zumino, Nucl. Phys. **B70** (1974) 39; H.P. Nilles, Phys. Rep. **110** (1984) 1; H.E. Haber and G.L. Kane, Phys. Rep. **117** (1985) 75; M.F. Sohnius, Phys. Rep. **128** (1985) 39.
- [9] For pedagogic introductions see e.g., M. Drees, R.M. Godbole and P. Roy, “*Theory and phenomenology of sparticles*”, World Scientific, 2005; H. Baer and X. Tata, “*Weak scale Supersymmetry: From superfields to scattering events*”, Cambridge University Press, 2006.
- [10] A. Djouadi, Phys. Rept. **459** (2008) 1 [hep-ph/0503173].
- [11] A.D. Sakharov, ZhETF Pis'ma **5** (1996) 32 (JETP Letters **5** (1967) 24).
- [12] For a review, see, E. Accomando et al., Workshop on CP studies and non-standard Higgs physics, CERN-2006-009 [hep-ph/0608079] and references therein.
- [13] R. M. Godbole, S. Kraml, M. Krawczyk *et al.* [hep-ph/0404024]; an extended version of the report is given in Ref. [6].
- [14] B. Grzadkowski, J. F. Gunion, Phys. Lett. **B294** (1992) 361 [hep-ph/9206262].
- [15] J. R. Dell'Aquila, C. A. Nelson, Phys. Rev. **D33** (1986) 80; C. A. Nelson, Phys. Rev. **D37** (1988) 1220.
- [16] V. D. Barger, K. -m. Cheung, A. Djouadi, B.A. Kniehl and P.M. Zerwas, Phys. Rev. **D49** (1994) 79 [hep-ph/9306270]; M. Kramer, J. H. Kuhn, M. L. Stong and P.M. Zerwas, Z. Phys. **C64** (1994) 21 [hep-ph/9404280].
- [17] A. Skjold, P. Osland, Phys. Lett. **B311** (1993) 261 [hep-ph/9303294].
- [18] S. Y. Choi, D. J. Miller, 2, M. M. Mühlleitner and P.M. Zerwas, Phys. Lett. **B553** (2003) 61 [hep-ph/0210077]; M. T. Dova, P. Garcia-Abia and W. Lohmann, [hep-ph/0302113]; C. P. Buszello, I. Fleck, P. Marquard and J.J. van der Bij, Eur. Phys. J. **C32** (2004) 209 [hep-ph/0212396]; C. P. Buszello, P. Marquard, J. J. van der Bij, [hep-ph/0406181]; Y. Gao, A. V. Gritsan, Z. Guo, K. Melnikov, M. Schulze, N. V. Tran, Phys. Rev. **D81** (2010) 075022 [arXiv:1001.3396 [hep-ph]]; C. Englert, C. Hackstein, M. Spannowsky, Phys. Rev. **D82** (2010) 114024 [arXiv:1010.0676 [hep-ph]]; U. De Sanctis, M. Fabbrichesi, A. Tonerio, [arXiv:1103.1973 [hep-ph]].
- [19] D. Chang, W. -Y. Keung, I. Phillips, Phys. Rev. **D48** (1993) 3225 [hep-ph/9303226].
- [20] A. Skjold, P. Osland, Phys. Lett. **B329** (1994) 305 [hep-ph/9402358].
- [21] E. Asakawa, S. Y. Choi, K. Hagiwara *et al.*, Phys. Rev. **D62** (2000) 115005 [hep-ph/0005313]; E. Asakawa, K. Hagiwara, Eur. Phys. J. **C31** (2003) 351 [hep-ph/0305323].
- [22] R. M. Godbole, S. D. Rindani and R. K. Singh, Phys. Rev. D **67** (2003) 095009, [Erratum-ibid. D **71** (2005) 039902], [arXiv:hep-ph/0211136].

- [23] S. Y. Choi, J. Kalinowski, Y. Liao, P. M. Zerwas, Eur. Phys. J. **C40** (2005) 555 [hep-ph/0407347].
- [24] P. Niezurawski, A. F. Zarnecki and M. Krawczyk, Acta Phys. Polon. B **36** (2005) 833, [arXiv:hep-ph/0410291].
- [25] R. M. Godbole, S. Kraml, S. D. Rindani and R. K. Singh, Phys. Rev. D **74** (2006) 095006 [Erratum-ibid. D **74** (2006) 119901] [arXiv:hep-ph/0609113]; R. M. Godbole, S. Kraml, S. D. Rindani and R. K. Singh, Pramana **69** (2007) 771.
- [26] R. M. Godbole, D. J. Miller, 2, M. M. Muhlleitner, JHEP **0712** (2007) 031 [arXiv:0708.0458 [hep-ph]].
- [27] A. De Rujula, J. Lykken, M. Pierini, C. Rogan, M. Spiropulu, Phys. Rev. **D82** (2010) 013003 [arXiv:1001.5300 [hep-ph]].
- [28] R. M. Godbole, P. Roy, Phys. Rev. Lett. **50** (1983) 717.
- [29] K. Hagiwara, M. L. Stong, Z. Phys. **C62** (1994) 99 [hep-ph/9309248].
- [30] D. J. Miller, 2, S. Y. Choi, B. Eberle, M.M. Mühlleitner and P.M. Zerwas, Phys. Lett. **B505** (2001) 149 [hep-ph/0102023].
- [31] G. J. Gounaris, F. M. Renard, N. D. Vlachos, Nucl. Phys. **B459** (1996) 51 [hep-ph/9509316]; A. Skjold, P. Osland, Nucl. Phys. **B453** (1995) 3 [hep-ph/9502283]; K. Hagiwara, S. Ishihara, J. Kamoshita and B.A. Kniehl, Eur. Phys. J. **C14** (2000) 457 [hep-ph/0002043]; T. Han, J. Jiang, Phys. Rev. **D63** (2001) 096007 [hep-ph/0011271].
- [32] S. S. Biswal, R. M. Godbole, R. K. Singh *et al.*, Phys. Rev. **D73** (2006) 035001 [hep-ph/0509070]; S. S. Biswal, D. Choudhury, R. M. Godbole *et al.*, Pramana **69** (2007) 777; S. S. Biswal, D. Choudhury, R. M. Godbole *et al.*, [arXiv:0710.2735 [hep-ph]]; S. S. Biswal, D. Choudhury, R. M. Godbole *et al.*, Phys. Rev. **D79** (2009) 035012 [arXiv:0809.0202 [hep-ph]]; S. S. Biswal, R. M. Godbole, Phys. Lett. **B680** (2009) 81 [arXiv:0906.5471 [hep-ph]].
- [33] K. Rao, S. D. Rindani, Phys. Lett. **B642** (2006) 85 [hep-ph/0605298]; K. Rao, S. D. Rindani, Phys. Rev. **D77** (2008) 015009 [arXiv:0709.2591 [hep-ph]]; S. D. Rindani, P. Sharma, Phys. Rev. **D79** (2009) 075007 [arXiv:0901.2821 [hep-ph]]; S. D. Rindani, P. Sharma, Phys. Lett. **B693** (2010) 134 [arXiv:1001.4931 [hep-ph]]; S. D. Rindani, P. Sharma, [arXiv:1007.3185 [hep-ph]].
- [34] T. Plehn, D. L. Rainwater, D. Zeppenfeld, Phys. Rev. Lett. **88** (2002) 051801 [hep-ph/0105325]; V. Hankele, G. Klamke, D. Zeppenfeld *et al.*, Phys. Rev. **D74** (2006) 095001 [hep-ph/0609075].
- [35] K. Odagiri, JHEP **0303** (2003) 009 [hep-ph/0212215]; G. Klamke and D. Zeppenfeld, JHEP **0704** (2007) 052 [hep-ph/0703202]; F. Campanario, M. Kubocz, D. Zeppenfeld, [arXiv:1011.3819 [hep-ph]].
- [36] V. Del Duca, G. Klamke, D. Zeppenfeld *et al.*, JHEP **0610** (2006) 016 [hep-ph/0608158]; J. R. Andersen, K. Arnold, D. Zeppenfeld, JHEP **1006** (2010) 091 [arXiv:1001.3822 [hep-ph]].

- [37] B. Badelek *et al.* [ ECFA/DESY Photon Collider Working Group Collaboration ], Int. J. Mod. Phys. **A19** (2004) 5097 [hep-ex/0108012].
- [38] B. Grzadkowski, J. F. Gunion, Phys. Lett. **B350** (1995) 218 [hep-ph/9501339].
- [39] W. Bernreuther, A. Brandenburg, Phys. Lett. **B314** (1993) 104 and Phys. Rev. **D49** (1994) 4481 [hep-ph/9312210]; W. Bernreuther, A. Brandenburg, M. Flesch, Phys. Rev. **D56** (1997) 90 [hep-ph/9701347].
- [40] W. Bernreuther, A. Brandenburg, M. Flesch, [hep-ph/9812387].
- [41] S. Bar-Shalom, D. Atwood, G. Eilam *et al.*, Phys. Rev. **D53** (1996) 1162 [hep-ph/9508314]; S. Bar-Shalom, [hep-ph/9710355]; D. Atwood, S. Bar-Shalom, G. Eilam, A. Soni, Phys. Rept. **347** (2001) 1 [hep-ph/0006032].
- [42] J. F. Gunion, X. -G. He, Phys. Rev. Lett. **76** (1996) 4468 [hep-ph/9602226].
- [43] J. F. Gunion, B. Grzadkowski, X. -G. He, Phys. Rev. Lett. **77** (1996) 5172 [hep-ph/9605326].
- [44] P. S. Bhupal Dev, A. Djouadi, R. M. Godbole *et al.*, Phys. Rev. Lett. **100** (2008) 051801 [arXiv:0707.2878 [hep-ph]]; R. M. Godbole, P. S. Bhupal Dev, A. Djouadi *et al.*, [arXiv:0710.2669 [hep-ph]].
- [45] C. -S. Huang, S. -h. Zhu, Phys. Rev. **D65** (2002) 077702 [hep-ph/0111280].
- [46] W. Khater, P. Osland, Nucl. Phys. **B661** (2003) 209 [hep-ph/0302004].
- [47] G. R. Bower, T. Pierzchala, Z. Was *et al.*, Phys. Lett. **B543** (2002) 227 [hep-ph/0204292]; K. Desch, Z. Was, M. Worek, Eur. Phys. J. **C29** (2003) 491 [hep-ph/0302046]; K. Desch, A. Imhof, Z. Was *et al.*, Phys. Lett. **B579** (2004) 157 [hep-ph/0307331].
- [48] K. J. F. Gaemers, G. J. Gounaris, Phys. Lett. **B77** (1978) 379; A. Djouadi, J. Kalinowski, P. M. Zerwas, Mod. Phys. Lett. **A7** (1992) 1765; A. Djouadi, J. Kalinowski, P. M. Zerwas, Z. Phys. **C54** (1992) 255; B. Grzadkowski, J. F. Gunion, J. Kalinowski, Phys. Rev. **D60** (1999) 075011 [hep-ph/9902308].
- [49] S. Dawson, L. Reina, Phys. Rev. **D57** (1998) 5851 [hep-ph/9712400] and **D59** (1999) 054012 [hep-ph/9808443]; S. Dittmaier, M. Kramer, Y. Liao *et al.*, Phys. Lett. **B441** (1998) 383 [hep-ph/9808433].
- [50] S. Dawson, L. Reina, Phys. Rev. **D60** (1999) 015003 [hep-ph/9812488]; S. Dittmaier, M. Kramer, Y. Liao *et al.*, Phys. Lett. **B478** (2000) 247 [hep-ph/0002035].
- [51] S. -h. Zhu, [hep-ph/0212273].
- [52] Y. You, W. -G. Ma, H. Chen, R. -Y. Zhang, S. Yan-Bin, H. -S. Hou, Phys. Lett. **B571** (2003) 85 [hep-ph/0306036]; G. Belanger, F. Boudjema, J. Fujimoto, T. Ishikawa, T. Kaneko, K. Kato, Y. Shimizu, Y. Yasui, Phys. Lett. **B571** (2003) 163 [hep-ph/0307029]; A. Denner, S. Dittmaier, M. Roth *et al.*, Phys. Lett. **B575** (2003) 290 [hep-ph/0307193] and Nucl. Phys. **B680** (2004) 85 [hep-ph/0309274].

- [53] S. Moretti, Phys. Lett. **B452** (1999) 338 [hep-ph/9902214]; A. Juste, G. Merino, [hep-ph/9910301]; M. Martinez, R. Miquel, Eur. Phys. J. **C27** (2003) 49 [hep-ph/0207315]; A. Gay, LCNote 2004; K. Desch and M. Schumacher in Ref. [6].
- [54] E. Boos, A. Djouadi, M. Muhlleitner *et al.*, Phys. Rev. **D66** (2002) 055004 [hep-ph/0205160].
- [55] T. Hayashi, Y. Koide, M. Matsuda *et al.*, Phys. Lett. **B348** (1995) 489 [hep-ph/9410413].
- [56] D. Zeppenfeld, R. Kinnunen, A. Nikitenko *et al.*, Phys. Rev. **D62** (2000) 013009 [hep-ph/0002036]; M. Dührssen, S. Heinemeyer, H. Logan *et al.*, Phys. Rev. **D70** (2004) 113009 [hep-ph/0406323]; M. Dührssen, S. Heinemeyer, H. Logan *et al.*, [hep-ph/0407190].
- [57] P. Garcia-Abia, W. Lohmann, Eur. Phys. J. direct **C2** (2000) 2 [hep-ex/9908065]; M. Battaglia, [hep-ph/9910271].
- [58] J. F. Gunion, H. E. Haber, J. Wudka, Phys. Rev. **D43** (1991) 904.
- [59] A. Mendez, A. Pomarol, Phys. Lett. **B272** (1991) 313.
- [60] J. F. Gunion, H. E. Haber and C. Kao, Phys. Rev. **D46** (1992) 2907.
- [61] W. Bernreuther, P. Gonzalez, M. Wiebusch, Eur. Phys. J. **C69** (2010) 31 [arXiv:1003.5585 [hep-ph]].
- [62] B. Grzadkowski and Z. Hioki, Phys. Lett. **B476** (2000) 87 [arXiv:hep-ph/9911505]; S. D. Rindani, Pramana **54** (2000) 791 [arXiv:hep-ph/0002006]; B. Grzadkowski and Z. Hioki, Phys. Lett. **B529** (2002) 82 [arXiv:hep-ph/0112361] and Phys. Lett. **B557** (2003) 55 [arXiv:hep-ph/0208079]; Z. Hioki, arXiv:hep-ph/0104105 and arXiv:hep-ph/0210224; K. Ohkuma, Nucl. Phys. Proc. Suppl. **111** (2002) 285 [arXiv:hep-ph/0202126]; R. M. Godbole, S. D. Rindani, R. K. Singh, JHEP **0612** (2006) 021 [hep-ph/0605100].
- [63] E. Accomando *et al.* [CLIC Physics Working Group Collaboration], [hep-ph/0412251].
- [64] U. Baur, A. Juste, L. H. Orr *et al.*, Phys. Rev. **D71** (2005) 054013 [hep-ph/0412021].
- [65] F. Larios, C. P. Yuan, Phys. Rev. **D55** (1997) 7218 [hep-ph/9606397]; W. Hollik, J. I. Illana, S. Rigolin *et al.*, Nucl. Phys. **B551** (1999) 3 [hep-ph/9812298].